Charles University

Faculty of Science

Study programme: Hydrology and Hydrogeology

Matouš Gottvald

Percolation column tests and investigation of contaminant leaching from mineral wastes: theory and experiment with metallurgical slag

Perkolační kolonové testy a studium vyluhovatelnosti kontaminantů z minerálních odpadů: teorie a experiment na metalurgické strusce

Type of thesis

Bachelor´s thesis

Supervisor:

prof. RNDr. Vojtěch Ettler, Ph.D.

Prague, 2023

Univerzita Karlova

Přírodovědecká fakulta

Studijní program: Hydrologie a hydrogeologie

Matouš Gottvald

Perkolační kolonové testy a studium vyluhovatelnosti kontaminantů z minerálních odpadů: teorie a experiment na metalurgické strusce

Percolation column tests and investigation of contaminant leaching from mineral wastes: theory and experiment with metallurgical slag

Typ závěrečné práce:

Bakalářská práce

Vedoucí práce/Školitel:

prof. RNDr. Vojtěch Ettler, Ph.D.

Praha, 2023

Zadání bakalářské práce

Název práce

Perkolační kolonové testy a studium vyluhovatelnosti kontaminantů z minerálních odpadů: teorie a experiment na metalurgické strusce

Student

Matouš Gottvald

Vedoucí/Školitel

prof. RNDr. Vojtěch Ettler, Ph.D.

Předběžná náplň práce dle SIS

Práce bude obsahovat jak rešeršní část týkající se kolonových testů aplikovaných na různé typy minerálních odpadů - důlní odpady, popílky, škváry (kompilace informací z odborné literatury), tak i experimentální část. V praktické části práce bude proveden laboratorní kolonový test na olovářské strusce za účelem zjištění vyluhovatelnosti kontaminantů (zejména Pb, Zn, As, Sb). Budou popsány geochemické procesy určující jejich mobilizaci. Práce bude navazovat na dlouhodobý perkolační experiment, který provádí školitel a bude navazovat po dlouhodobém (dvouměsíčním) přerušení experimentu tak, aby bylo možné ověřit vliv vysušení vzorku na změnu výluhových charakteristik (tzv. wetting-drying cycles).

Datum zadání práce: 13. 6. 2022

Podpis studenta:

Podpis vedoucího práce:

Declaration of Authorship

1. The author hereby declares that he compiled this thesis independently, using only the listed resources and literature.
2. The author hereby declares that all the sources and literature used have been properly cited.
3. The author hereby declares that the thesis has not been used to obtain a different or the same degree.

Prague 25th July 2023

Prohlášení

Prohlašuji, že jsem závěrečnou práci zpracoval samostatně a že jsem uvedl všechny použité informační zdroje a literaturu. Tato práce ani její podstatná část nebyla předložena k získání jiného nebo stejného akademického titulu.

V Praze, 25. 7. 2023   ………………………

                                                                    Matouš Gottvald

Acknowledgements

Poděkování

Abstract

Leaching represents an essential concept related to the natural processes that occur at the contact between solids and solutions. The leaching properties of mineral wastes point to the mobility of contained contaminants in various scenarios and, thus, the environmental risk of the wastes. Experimental tools have been developed to determine the leachability over a range of conditions and to be a part of the waste evaluation workflow. Special emphasis is given to the dynamic column leaching tests that approximate percolation occurring in the field and enable to describe the time dependence of leaching. Processes that are observed in full-scale systems may substantially differ from those in the laboratory simulations. Apart from the field experiments and geochemical modelling, also modifying the original leaching test protocols expands our awareness of the mineral waste behaviour. We performed a column leaching test. Secondary Pb metallurgical slag coming from the Pb-scrap recycling was leached according to the standardised column leaching test EN 14405 as a part of broader research on the leachability of slag exposed to the wetting-drying cycles. The cumulative leached mass of both metal and major elements was lower compared to the previous turn; bulk leached masses of the main contaminants related to the sample mass were on average (µg/kg): Ba 6743, Sb 221, Pb 47 and Zn 21. The highest concentrations of most constituents were observed at the beginning of the experiment. The concentration of none of the contaminants exceeded the threshold for hazardous waste; hydrous ferric oxides (HFO), baryte ($BaSO_4$) and cerussite ($PbCO_3$), which were already partially formed during the first part of the experiment are expected to control the release of toxic metal(loid)s. The equilibration of the column before the restart of the second experiment caused higher initial concentrations of constituents whose transport is mostly controlled by diffusion (and can be limited by physical non-equilibrium) compared to the last eluate fractions of the first run of the experiment.

Abstrakt

Loužení je základním konceptem v rámci přírodních procesů odehrávajících se na styku pevných látek a vody. Loužicí vlastnosti minerálních odpadů poukazují na mobilitu v nich obsažených kontaminantů při různých scénářích, a tedy na míru jejich nebezpečnosti pro životní prostředí. Byly vyvinuty experimentální nástroje k určení vyluhovatelnosti odpadového materiálu, které slouží jako jeden ze vstupů při klasifikaci odpadů dle nebezpečnosti. Zvláštní důraz je kladen na dynamické kolonové loužicí testy, které nejvěrněji simulují perkolaci, jakožto přirozený loužicí proces v terénních podmínkách, a které umožňují popsat závislost vyluhování na čase. Procesy pozorované v terénu se mohou podstatně lišit od procesů v laboratorních simulacích. Tyto simulace je žádoucí doplnit daty z terénních experimentů a geochemického modelování či modifikovat původní protokoly loužicích testů. Jako součást práce byl proveden kolonový test podle normy EN 14405 na sekundární Pb metalurgické strusce pocházející z recyklace olověných akumulátorů. Jednalo se o další v řadě experimentů v rámci déle trvajícího výzkumu vyluhovatelnosti této strusky v případě tzv. wetting-drying cycles. Celkové vyluhované hmotnosti kovů i hlavních prvků byly v porovnání s předchozím během experimentu nižší, celkové hmotnosti nejdůležitějších vyluhovaných kontaminantů byly v průměru (µg/kg): Ba 6743, Sb 221, Pb 47 a Zn 21. Nejvyšších koncentrací většiny vyluhovaných látek bylo dosaženo na počátku experimentu. Žádná z koncentrací kontaminujících látek nepřekročila prahovou hodnotu pro nebezpečný odpad; předpokládáme, že toxické (polo)kovy byly zadrženy hydratovanými oxidy železa (HFO), barytem ($BaSO_4$) a cerusitem ($PbCO_3$), které se již částečně vysrážely během první části experimentu. Ekvilibrace strusky s loužicím roztokem, která předcházela opětovnému spuštění kolonového experimentu způsobila vyšší počáteční koncentrace složek, jejichž transport závisí zejména na difuzi (a může být omezen fyzikální nerovnováhou), v porovnání s posledními frakcemi výluhu v první části experimentu.

List of contents

1. Introduction

Waste materials may contain toxic substances that potentially pose a danger to humans and the environment. In order to prevent harmful environmental impacts, it is necessary to characterise these wastes and estimate their behaviour under specific conditions corresponding to a given environmental scenario (Kosson et al., 2002, 2014). Mineral wastes particularly discussed in this bachelor thesis are either deposited in a disposal site or subsequently used (e.g., for engineering purposes, for instance, as an additive into construction materials) (Fällman and Hartlén, 1994; Kosson et al., 2002, 2014). Municipal solid waste incineration (MSWI) wastes, such as bottom ash (BA) or fly ash (FA), various slags, mattes and waste rock, are examples of mineral wastes whose environmental assessment is needed.

The basic questions concerning the waste classification include how stable the material is when it is exposed to outdoor conditions during the interaction with the rain or the groundwater; and how mobile are the contained contaminants. Normalised laboratory procedures designed to characterise the degree of materials' hazardousness provide a partial view of the complex behaviour of mineral wastes in field conditions (Kosson et al., 2014).

The aim of this bachelor thesis is (i) to describe the ways of determining the leachability of contaminants that are contained in mineral wastes, with an emphasis on the dynamic leaching experiments and, (ii) to assess the leachability of contaminants from a specific mineral waste using a laboratory dynamic leaching experiment. A secondary Pb slag used as an example material in this work will be subject to a column leaching test according to EN 14405 (2017) to determine the behaviour patterns of the slag in contact with water, which will be simultaneously appraised in the context of the preceding column experiment conducted on the same waste material up to liquid-to-solid ratio of 30. The influence of drying the material and restarting the water percolation on the constituent mobility during the wetting-drying cycles is of crucial importance.

2. Current state of knowledge

2.1 Leaching processes

To obtain a waste environmental assessment, a process called *leaching* is broadly applied in the form of laboratory leaching tests (Zhang et al., 2001). Leaching, which is defined as a release of constituents from the solid substance in contact with a liquid phase (water), is considered an important natural mechanism of component mobilisation by both chemical (e.g., dissolution, desorption, complexation) and mass transport processes (LEAF, 2022). The bulk chemical composition of the leached material is definitely not the only factor determining leachability (Hyks et al., 2009b; Ettler and Vítková, 2021), and it is incorrect to presume that the total content of a contaminant is available for release (Kosson et al., 2002). Primarily, the *liquid-solid partitioning* (LSP), along with the physical properties of the material (particle size ~ specific surface area exposed (Ettler and Vítková, 2021)), the degree of equilibrium and the liquid phase qualities determine the leaching rates. The main LSP drivers include pH (governing also consequent geochemical processes), ionic strength, complexation possibilities and redox (Kosson et al., 2014); moreover, the LSP naturally depends on the mineralogical composition. The overview of geochemical processes at the solid phase-water interface is presented in Figure 1.

2.1.1 Leaching tests

The leaching tests may be defined as sets of given work procedures determining the material's leachability through the composition of final eluate or eluate fractions separated in the course of the experiment. Thus, in conjunction with other inputs, the tests may be used to estimate the leaching properties of the waste under various management scenarios and assess its environmental impact during deposition or secondary reuse. In some countries, the leaching tests are enrooted in the legislation concerning waste management and are used as a decision tool for waste classification (Kosson et al., 2002). In the European Union, leaching tests belong to a set of standards headed by CEN/TC 444 – Environmental characterization of solid matrices, designed by CEN (European Committee for Standardization); in the USA, they come under SW-846 – Test Methods for Evaluating Solid Wastes established by US EPA (US Environmental Protection Agency).

Based on the renewal of the leaching solution, leaching tests can be either *static* or *dynamic*, barring a special category of *semi-dynamic* tests (Kosson et al., 2014). All these types of leaching tests are characterised in the chapters below.
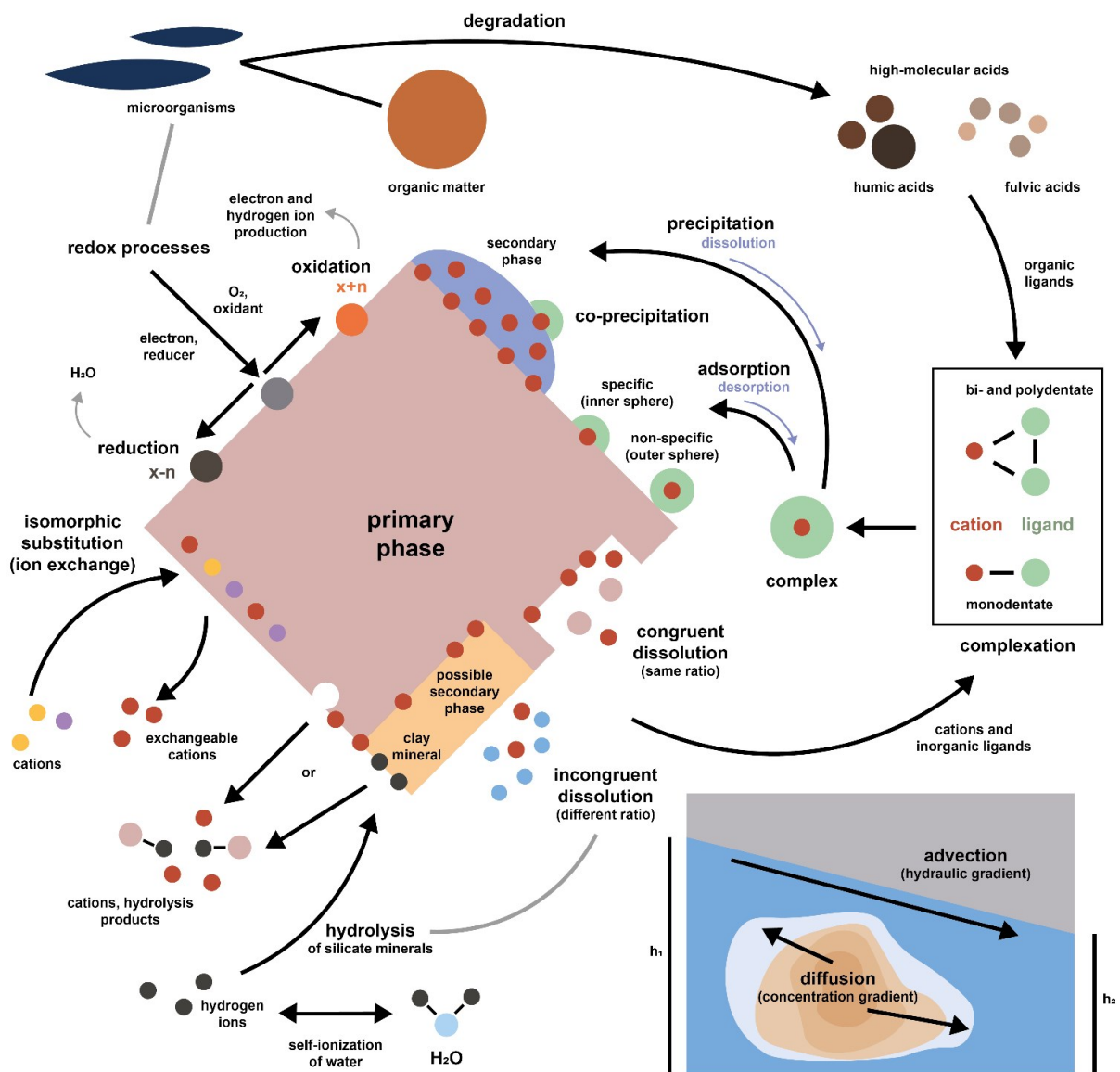
Figure 1. The geochemical processes and transport mechanisms associated with leaching.

2.2 Static and semi-dynamic leaching tests

2.2.1 Static leaching tests

In the case of static (batch) leaching tests, the leaching solution is not refreshed over time, and the equilibrium between the solid and the liquid phase is expected to be reached (Kosson et al., 2014); this usually occurs in a short period because of the initial steep concentration gradients between the phases (Grathwohl and Susset, 2009). This period corresponds to the duration of most batch tests. That is why static tests are also called equilibrium-based (Kosson et al., 2014). The system comes to equilibrium at the moment the mass transfer is suspended (Grathwohl and Susset, 2009).

Short-term *batch tests* represent the simplest leaching method designed for granular materials. The waste material is placed in a vessel upon contact with distilled water at an exact *L/S ratio* (*liquid* mass to *dry solid* mass, expressed typically in mL/g or L/kg) (Kosson et al., 2014) while the pH of the *leachant* (i.e., leaching solution) is not controlled and is dictated by the solid phase itself (Fällman and Hartlén, 1994). Carrying out a batch test usually takes a maximum of a few days (Ettler and Vítková, 2021), and its price is relatively low (V. Ettler, pers. commun., 2022). Nevertheless, the results provided are rather limited. For example, we cannot observe long-term interactions between the solid and the liquid phase (van der Sloot et al., 2001; Ettler and Vítková, 2021). Widely used normalised batch extraction procedures compiled under the European norm EN 12457 (parts 1–4, 2002; the parts are listed in Table 1) and analogically Test Method 1316 (2017) by US EPA both express leachability of the constituents as a function of L/S ratio.

Table 1. Overview of the methods compiled under the European norm EN 12457.

Part number	Number of stages	L/S ratio (L/kg)	Max. particle size (mm) – with or without size reduction
1	one stage	2	<4
2	one stage	10	<4
3	two stages	2 and 8	<4
4	one stage	10	<10

The *pH-dependent parallel batch tests* expressing the extent of release as a function of the final eluate's pH are of major importance because, as mentioned above, pH is considered the main driver of liquid-solid partitioning within the equilibrium state influencing fundamentally the form of a given constituent in the system (Kosson et al., 2014). European EN 14429 (2015) (or EN 14997 (2015)) and similarly Test Method 1313 (2017) represent parallel batch extraction procedures where the assessed waste is leached under the range of different pH conditions at L/S of 10 covering values from strongly acidic to strongly alkaline conditions. For Test Method 1313 (2017), there are 8 set pH values between 2 and 13 plus batch reactor corresponding to a natural pH of the sample; for EN 14429/14997, at least 8 pH values

have to be selected to cover the pH range 4–12. Within EN 14429 (2015), the pH drifts spontaneously after the initial pH adjustment (up to the selected values) achieved by the acid/base addition. The amount of acid or base depends on the preliminary acid/base neutralisation capacity (ANC/BNC) of the material (Ettler and Vítková, 2021). In contrast, pH is continuously controlled for the whole duration of the test EN 14997 (2015).

Figure 2 shows a dependence of Cd release on pH, matching the pH intervals to the particular environmental scenarios. The 8 points representing batch experiments within the pH range defined by EN 14429 (2015) cover most of these scenarios. The simultaneously obtained data from EN 12457-2 are recorded as well. Although it is not so likely that more extreme pH values will be reached in the field, it can be useful to identify the pH interval at which the material releases the highest amounts of
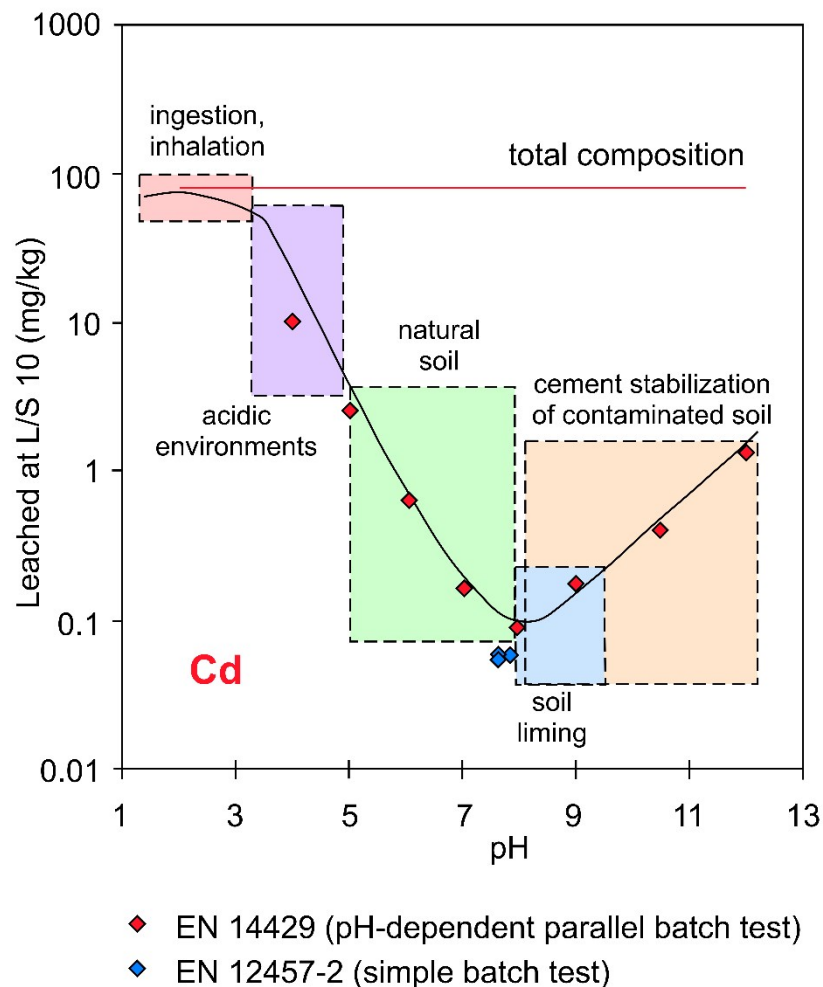

Figure 2. The relevance of leaching showed in the example of the pH-dependent behaviour of a sewage sludge-amended soil. Individual pH intervals correspond to the environmental scenarios to which the waste may be exposed. The points represent leaching data obtained from the mentioned European norms (modified from Leaching.net, 2007).

potentially toxic elements (van der Sloot et al., 2001). Also, the pH-dependent tests are suitable tools for comparing the leaching behaviour between different mineral residues (van der Sloot et al., 2001; Kosson et al., 2014) and for subsequent hydrogeochemical modelling (Ettler and Vítková, 2021).

2.2.2 Semi-dynamic leaching tests

For the monolithic or compacted materials with low permeability (deposited, e.g., in the vadose zone), the mass transport (i.e., a combination of diffusion inside the pores of the monolith and partitioning at the solid-liquid interface) is the limiting factor of release of constituents (Garrabrants et al., 2014, 2021; Ettler et al., 2023). The leached elements get through the pore network of the monolith to the surface, being driven by the concentration gradient. Therefore, the *mass transfer-based leaching tests* are set as semi-dynamic, preventing concentration gradient decrease over time. Concentration gradient preservation is achieved by renewing the leachant in predefined time intervals (Kosson et al., 2014). That corresponds to the cycles occurring in the field – each infiltration event represents a concentration gradient resumption. Thus, during the cycles the cumulative mass released is greater than during continuous release. The estimates provided by these tests tend to be conservative (showing rather overestimated release) because the infiltration is significantly limited in the field conditions (Garrabrants et al., 2021). Test Method 1315 (2017) and EN 15863 (2015) are examples of existing mass transfer-based tests used in practice.

2.3 Dynamic leaching tests

In the dynamic tests, the granular waste is leached under *hydraulically dynamic conditions*, i.e., the leaching solution percolates through the layer of material at a specified flow rate (EN 14405, 2017). Percolation represents a principal leaching mechanism in nature (Grathwohl and Susset, 2009) since a part of rainwater infiltrates and passes through the ground. Accordingly, dynamic leaching is regarded as a suitable tool for estimating leachate constituent concentrations likely obtained in a scenario supposing slow percolation through a permeable material (Kosson et al., 2014; Souter and Watmough, 2017). The following chapters are devoted to this type of leaching test, being the major focus of this bachelor thesis.

2.3.1 Column tests

The commonest implementation of dynamic leaching is percolation through a vertical column filled with the examined material. In general, the term *column leaching test* or *percolation test* is used as a synonym for a dynamic leaching test. Deionised water propelled by a volumetric pump continuously percolates through the granular material up to a desired volume characterised by an L/S ratio, usually in the up-flow mode with the purpose of avoiding channelling along the side of the cylinder (Kosson et al., 2014; EN 14405, 2017), preferential flow inside the filling (EN 14405, 2017) and air capturing (Grathwohl and Susset, 2009; Kosson et al., 2014). In contrast to the static leaching test, where only the final eluate can be analysed, several individual fractions corresponding to defined L/S ratios are sampled in the course of the test, more frequently during the beginning of the experiment. Assuming local equilibrium (see below), the sample corresponds to an average constituent release during the interval between the two L/S values. The final leachate concentration of individual constituents can thus be expressed as a function of cumulative L/S ratio (example in Figure 3) (Kosson et al., 2014), which means that the concentrations obtained from the individual fractions are summed successively and plotted against the growing L/S ratio where the value at the end of the experiment tallies the total amount of constituent released.
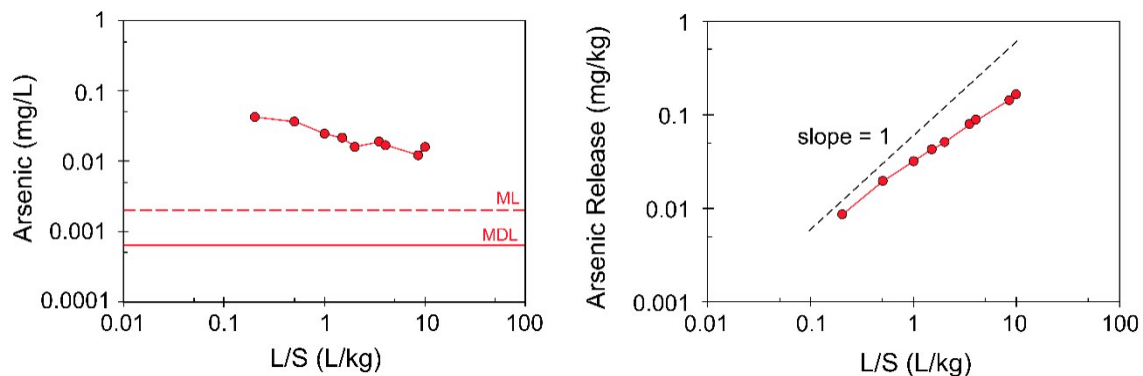

Figure 3. Aqueous concentrations of arsenic (As) plotted against L/S ratio. On the left, amounts of As leached in the individual eluate fractions, on the right, cumulative release of As as a function of the L/S ratio. Example from Test Method 1314 results (modified from Kosson et al., 2014).

2.3.2 The relationship between L/S ratio and time

Depending on the net infiltration, the L/S ratio corresponds to the time at which the same volume of infiltrated water passes through the material under the field conditions, also taking into account the bulk density and the thickness of the layer of the material. Van der Sloot et al. (2001) define the relationship between the L/S ratio reached during a column leaching test (in L/kg) and time (1) as follows:

$$L / S = I \cdot t / (\rho \cdot h) \quad (1)$$

where I stands for the net infiltration in mm/year, t for the time in years, ρ is the bulk density of the dry material in kg/m³, and h corresponds to the height of the material in the column (or at a waste disposal site) in m.

For instance, the course of the eluate concentrations obtained by leaching a 0.5 m layer of the MSWI residue with the bulk density of 4000 kg/m³ up to an L/S ratio of 10 would simulate the behaviour of the waste over the period of 100 years of open storage when counting on the infiltration of 200 mm/year (van der Sloot et al., 2001; Hyks et al., 2009b). To shorten the laboratory experiment duration, the linear velocity (independent of pore volume) is set significantly higher compared to natural infiltration, and an L/S ratio of 10 may be reached within approximately 30 days (EN 14405, 2017). According to van der Sloot et al. (2001), the hydraulic retention time is not a deciding parameter for the constituent amount leached, and thus, the column tests can representatively simulate a natural infiltration scenario in a short time. However, the appropriate contact time (to approximate the equilibrium) is strictly related to the particle size and the sample size (Kosson et al., 2002).

2.3.3 Equilibrium and non-equilibrium

As reported by Kosson et al. (2014), "percolation tests carried out at relatively slow flow conditions (…) approximate *local equilibrium* between the pore solution and the solid phase at any given point in the column". The equilibrium is an important assumption required if the partitioning processes and solid phase controls are to be modelled (Hyks et al., 2009a).

In fact, the local equilibrium is usually reached only at the beginning of a column experiment, subsequently replaced by non-equilibrium conditions (Grathwohl and Susset, 2009). That raises the question of whether results from a dynamic experiment can be relevant inputs for geochemical speciation modelling; nonetheless, according to Grathwohl and Susset (2009), the theoretical calculations assuming equilibrium and the column test results agree surprisingly well.

Physical non-equilibrium manifests by a prolonged decrease in concentrations of *availability-controlled* constituents called *tailing*. The transport of these constituents is mostly influenced by diffusion, which can be slowed down owing to the dual-porosity effect (the diffusion between the inside of a particle and its surface is limited compared to the swift diffusion among the particles), resulting in physical non-

equilibrium (Hyks et al., 2009a). Contrarily, under conditions close to equilibrium observed in the field, these elements or compounds (often seen as readily-soluble, e.g., dissociated salts) are generally washed away in the initial stage of leaching, followed by their depletion (Hyks et al., 2009a, b; Kosson et al., 2014). Furthermore, Hyks et al. (2009a) describe a chemical non-equilibrium. The solubility kinetics of some *solubility-controlled* constituents (for instance, Ca, Al, Ba, SO_4^{2-}, metals) is relatively slow compared to a column test (Hyks et al., 2009a) whose infiltration rate is substantially accelerated relative to the field infiltration (Hyks et al., 2009a; EN 14405, 2017). At the moment the flow is interrupted, increased eluate concentrations of contaminants can be observed despite comparatively stable pH as the time for the equilibration is longer (Hyks et al., 2009a). Solubility-controlled elements are distinguished by relatively steady release throughout the leaching period (Hyks et al., 2009b). Change to non-equilibrium may be caused by both outer influence alterations (flow velocity), the mass transport limitation related to the dual porosity effect (Grathwohl and Susset, 2009; Hyks et al., 2009a), the sorption capacity or the release kinetics of the observed material (Grathwohl and Susset, 2009).

2.3.4   *Comparison of column and batch tests*

Although batch and column leaching tests provide comparable results via the L/S-dependence plotting, there are some dissimilarities between these methods (Grathwohl and Susset, 2009). As said above, simple batch extraction tests are easy to accomplish; however, the obtained information on leaching is rather specific, referring to the only situation being simulated (van der Sloot et al., 2001). Therefore, column tests are considered more robust and are preferred (Grathwohl and Susset, 2009) primarily due to their ability to show temporal dependence of leaching rates by means of the sampled eluate fractions (Zhang et al., 2001). The dynamic of leaching is also closer to the actual percolation occurring under field conditions (Zhang et al., 2001; Grathwohl and Susset, 2009).

According to Grathwohl and Susset (2009), the total leachate concentrations obtained by column testing tend to be lower for greater L/S ratio values compared to the batch tests. This happens owing to the occurrence of non-equilibrium conditions in the later stages of the percolation experiments, which makes concentrations drop below the equilibrium level. On the contrary, during the initial stage of leaching (corresponding to lower L/S values), batch tests usually underestimate the release of various contaminants observed in field lysimeter leachates (e.g., chlorides). In contrast, the release simulated by column tests shows good agreement with field data (Grathwohl and Susset, 2009). Also, interactions between already-washed-out elements or compounds and the remaining solid phase are possible during a static batch test (van der Sloot et al., 2001). Van der Sloot et al. (2001) showed that during a column experiment conducted on an MSWI residue, mobilisation of Cd by chlorides was prevented due to the dynamic of leaching. The chlorides were washed away at the beginning of the experiment; however, Cd can be mobilised only under more acidic conditions, which were reached during the later stages of the experiment. The obtained release of Cd was, therefore, lower than it would have been expected based on the results of a static test (van der Sloot et al., 2001).

In the case of column tests, the composition of the leached material is changing with the amount of eluent passing through (Kosson et al., 2014). Discrete L/S intervals represented by the collected percolate fractions enable to observe the elution rates of the constituents individually, taking into account actual (pH) conditions (Kosson et al., 2014; Ettler and Vítková, 2021). In this way, the non-interacting species and the solubility-controlled species can be divided, and the solubility control information may be acquired (Ettler and Vítková, 2021). Contrarily, in a single final leachate obtained from a batch test an assemblage of leaching phenomena can hardly be distinguished.

2.3.5 Normalised column leaching procedure methodology

This subchapter is devoted to the detailed methodology of the normalised European percolation test EN 14405. Test Method 1314 (2017) protocol is highly similar as their development was interconnected.

A column made of glass or plastics with a height of 30 cm and an internal diameter of 5 or 10 cm (depending on the grain size fractions in the sample) is packed with granular material, which is enclosed between two filters on top and bottom sections represented by a filter plate or a fine quartz sand layer. If the analysed material is also coarse-grained, particle size reduction has to be carried out to homogenise the sample and simplify the establishment of the equilibrium; however, it is desirable not to do so (EN 14405, 2017). Such intervention can change the leaching properties of the examined sample because of the specific surface area augmentation, the opening of new surfaces not affected by natural weathering (EN 14405, 2017; Ettler and Vítková, 2021), and the disturbing the already-weathered ones (EN 14405, 2017). Crushing the sample may also lead to the formation of fine dust adhered to larger particles whose dissolution might then cause higher initial leaching (Vítková et al., 2011; Ettler and Vítková, 2021). If the dust is removed, e.g., ultrasonically in alcohol, a decrease in leaching can be expected (Seignez et al., 2008; Vítková et al., 2011). The rules for the size reduction depending on the fraction < 4 mm and ≥ 10 mm related to the type of column used (small or wide) are specified in the standard EN 14405 and are reported in Table 2. Generally, the sample has to be handled carefully to prevent chemical alterations that may occur, especially during its drying (EN 14405, 2017).

Table 2. Type of column used according to the particle size distribution (EN 14405, 2017).

Fraction < 4 mm	Fraction ≥ 10 mm	Column to be used (with required size reduction)
≥ 95 % (m/m)		Small column (without size reduction)
		or
		Wide column (without size reduction)
80 % (m/m) to 95 % (m/m)	≤ 5 % (m/m)	Small column (with size reduction of the fraction ≥ 4 mm)
		or
		Wide column (without size reduction)
≤ 80 % (m/m)	≤ 5 % (m/m)	Wide column (without size reduction)
	> 5 % (m/m)	Wide column (with size reduction of the fraction ≥ 10 mm)

Distilled water, used as a leachant, is propelled from the reservoir by a volumetric (peristaltic or similar) pump and percolates through the column, from the base upwards. The eluate is subsequently collected into collection bottles of volume corresponding to the currently sampled L/S fraction. The complete setup of the experiment is shown in Figure 4. The flow rate is adjusted so that linear velocity in the empty column reaches approximately 15 cm/day (EN 14405, 2017). By comparison, within Test Method 1314 (2017), the flow rate is expressed by means of the L/S ratio, reaching about 0.75 L/S per day. In both cases, the flow rate is low enough so that the local equilibrium might be approximated (EN 14405, 2017; Test Method 1314, 2017).

The column is saturated with water and left to equilibrate for a certain period (16 hours to 3 days) (EN 14405, 2017). The equilibration period is 18 to 24 hours for Test Method 1314 (2017). Alternatively, the "stationary" equilibration method can be substituted by circulating the eluent in a closed loop as long as pH is changing significantly (EN 14405, 2017; Test Method 1314, 2017).

After the equilibration period, the peristaltic pump is started, and fresh leachant (distilled water) enters the column (EN 14405, 2017). A preconditioned sample (15 mL at most) of pore water equilibrated with solid is then collected in order to check the value of pH (Grathwohl and Susset, 2009; EN 14405, 2017). If pH is higher than 9, the collection bottles for the following leachate fractions shall be kept under an inert atmosphere (of Ar or N_2, avoiding carbonation, see below). The first eluate portion at the L/S of 0.1 is sampled in a short time, preconditioned sample inclusive. In total, 7 percolate fractions corresponding to given L/S values have to be collected (EN 14405, 2017); the overview is reported in Table 3.
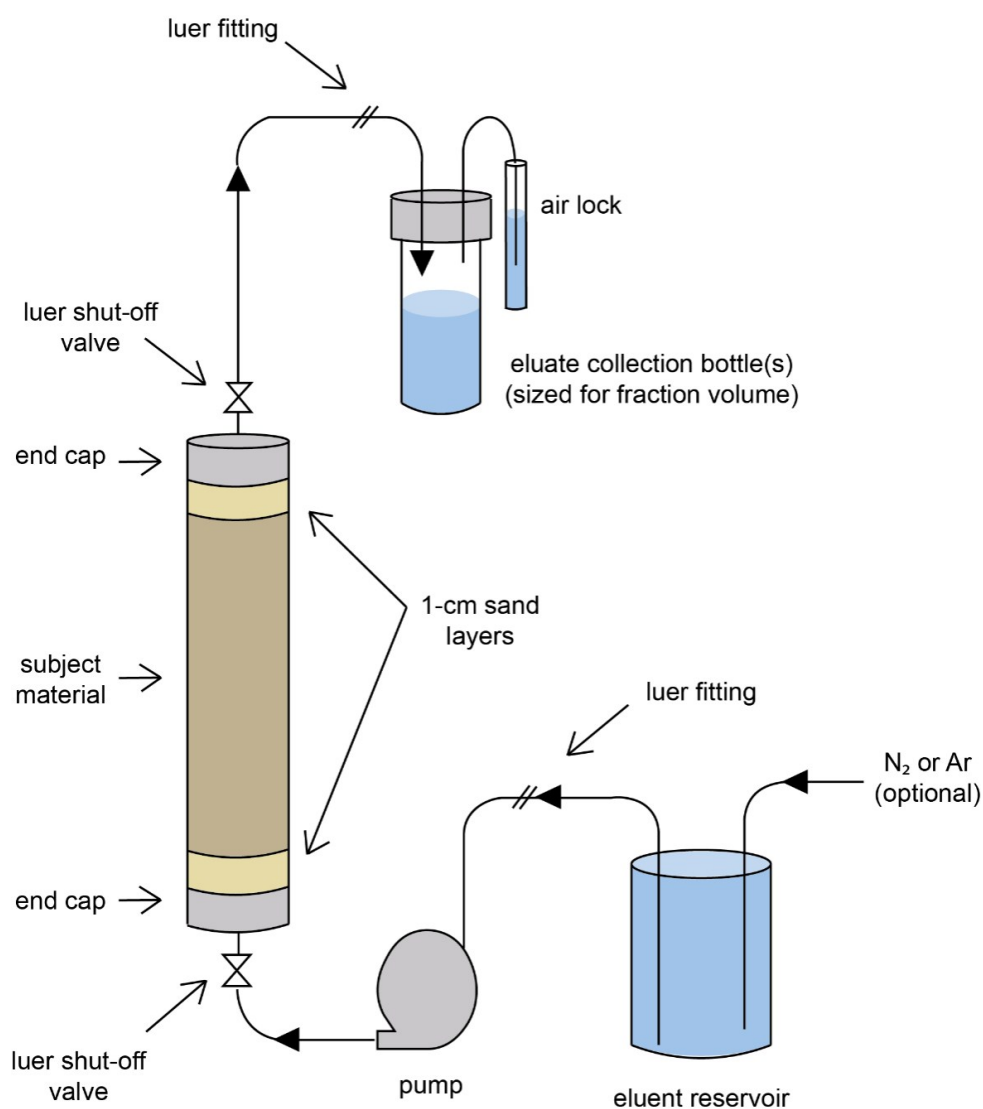
Figure 4. Column leaching test setup scheme (Test Method 1314, 2017).

Table 3. Overview of the sampled eluate fractions defined by the L/S ratio (EN 14405, 2017).

Fraction number	Fraction volume (= L/S ratio times dry mass)	Cumulative L/S ratio
	L	L/kg dry matter
1	$(0.1 \pm 0.02) \times m_0$	0.1 ± 0.02
2	$(0.1 \pm 0.02) \times m_0$	0.2 ± 0.04
3	$(0.3 \pm 0.05) \times m_0$	0.5 ± 0.08
4	$(0.5 \pm 0.1) \times m_0$	1.0 ± 0.15
5	$(1.0 \pm 0.2) \times m_0$	2.0 ± 0.3
6	$(3.0 \pm 0.2) \times m_0$	5.0 ± 0.4
7	$(5.0 \pm 0.2) \times m_0$	10.0 ± 0.1

Immediately after the eluate fraction collection, pH, Eh and specific conductivity are recorded, and the sample is filtered through a 0.45 μm membrane filter, after which is divided into sub-samples for the subsequent chemical analysis. These are subject to various characterisation methods determining bulk concentrations of individual constituents (major cations, anions and trace elements) and, in specific cases, also dissolved organic carbon (DOC) (EN 14405, 2017). Typically, inductively coupled plasma optical emission spectrometry (ICP-OES) and ICP mass spectrometry (ICP-MS) are used to measure major cations and trace elements, and liquid chromatography is adopted to measure anions (Ettler and Johan, 2014).

2.3.6 Modified column leaching experiments

Many researchers do not adopt the normalised leaching protocols unchanged; often, the column experiments are modified to better comply with the research objectives (Ettler and Vítková, 2021). Either the percolation reactors can be physically adjusted (dimensions, etc.), or the standard column is used, with changes e.g., in the duration (modifying the target L/S ratio) or the flow regime of the experiment.

Both Strömberg and Banwart (1999) and Souter and Watmough (2019) used custom-made columns open to the atmosphere to study the leaching parameters of some sulphide-containing materials (waste rock and Cu-Zn slag) that would be at least partially subject to oxidation under the field conditions. Apart from the difference in dimensions compared to the standard protocol (the mentioned researchers used large columns [2×0.8 m] and thin columns [35×3.8 cm], respectively), the percolation/irrigation regime was also altered. The up-flow mode was substituted by the gravitational flow; within the experiment carried out by Strömberg and Banwart (1999), the reactors irrigated by a sprinkler system simulating rainfall were used. By contrast, Souter and Watmough (2019) observed the influence of individual washing events on leaching, pouring a certain volume of water into the top of the column; the preferential flow paths were avoided owing to the layer of the glass balls distributing the flow equally.

Hyks et al. (2009b) have also adapted the EN 14405 leaching standard to study long-term leaching properties of MSWI air-pollution-control residues. The standard experiment period was extended to 24 months, reaching the L/S ratio values of 200–250, corresponding to more than 10 000 years of leaching in the field (Hyks et al., 2009b). The column test protocol was also altered within the MSWI bottom ash leaching experiment by Hyks et al. (2009a), who introduced a pair of flow interruptions at L/S = 2 and L/S = 12. The subsequent response in the leaching of individual constituents was described using more frequent sampling of the eluate after restarting the experiment at the end of the flow interruption interval (Hyks et al., 2009a).

2.4   Examples of column leaching from mineral wastes

The mineral wastes produced by mining, metal processing, municipal waste incineration or other industrial activities vary in both chemical and mineralogical composition which is narrowly connected to the way of their genesis. This short chapter aims to provide information about the column leaching characteristics of the most common mineral wastes except metallurgical slags, whose leaching patterns are described in detail in a special section.

2.4.1   MSWI bottom ash (BA)

Municipal solid waste incineration residues often do not meet the environmental criteria (van der Sloot et al., 2001), and there is a need for a precise assessment of their long-term behaviour if they are to be used for engineering purposes (Freyssinet et al., 2002; Hyks et a., 2009b). Bottom ash is characterised by its heterogeneity (van der Sloot et al., 2001, Hyks et al., 2009a), composed of fine soluble fraction (containing carbonates, sulphates, artificial phases and metallic micro-droplets) and coarser glassy silicate fraction, which also includes non-combustible remnants of original waste (e.g., bottle glass) (Hyks et al., 2009a). Despite relatively high contents of metals (low thousands of mg/kg) such as Pb, Zn, Cu or Ba (Fällman and Hartlén, 1994; Freyssinet et al., 2002; Hyks et al., 2009a), the high dissolution of readily-soluble salts represents the biggest problem (van der Sloot et al., 2001) resulting in fast initial leaching of Na^+, K^+ and Cl^-. In the column test by Hyks et al. (2009a), their first eluate concentrations reached 2000, 800 and 3000 mg/L, respectively. The majority of metals are solubility-controlled; carbonates are common controlling phases of Pb and Zn (Freyssinet et al., 2002; Hyks et al., 2009a). As mentioned above, Hyks et al. (2009a) examined the influence of flow interruptions during column leaching test on the release of various constituents from MSWI BA. Solution concentrations of solubility-controlled constituents were relatively stable, slightly changing during the flow interruption (for example, Ba and Al conc. increasing). The leaching of Cu, Ni and Mo was more significantly increased; for Cu and Ni, the complexation with DOC (whose diffusion was enhanced during the interruptions) has been suggested as the deciding mechanism of release. The absence of Mo-controlling phases and the lack of evidence for Mo complexation led to the conclusion Mo was simply controlled by diffusion from the stagnant zones in the MoO_4^{2-} form (Hyks et al., 2009a).

2.4.2   APC residues

Air pollution control (APC) residues are another waste materials from the MSW incineration or other combustion/high-temperature processes; they are produced during the cleaning of the flue gases (Hyks et al., 2009b) and are treated separately from the bottom ash (Fällman and Hartlén, 1994). These residues are fine dusty materials and are distinguished by higher natural pH compared to the MSWI BA; they also have higher contents of metals and readily-soluble salts which makes them even less stable and thus hazardous (Hyks et al., 2009b). Fly ash (FA) represents a pure not-treated APC residue; ash coming from the flue-gas cleaning, enriched in lime and acid gas neutralisation products, is called semi-dry (SD) residue in the work by Hyks et al., 2009b. Leaching of SD residues thus shows substantially higher

alkalinity, pH and conductivity compared to FA (Figure 5). Generally, the APC residues cannot be landfilled without a preceding treatment (van der Sloot et al., 2001; Hyks et al., 2009b). Their leaching is analogous to that of bottom ash; massive dissolution of salts (e.g., NaCl or KCl) at low L/S values (resulting in the increased initial leaching of Na, K and Cl depicted in Figure 5) with leaching of metals represent the most serious problems. Within a long-term column leaching up to the L/S of 200-250 L/kg performed by Hyks et al. (2009b), substantial amounts of Ba (149 and 39 mg/kg), Sr (355 and 164 mg/kg) and Mo (3 and 9 mg/kg), were released from the SD residue and FA respectively. Less than 3 % of the total contents of most metals were released during the two years of column leaching (Hyks et al., 2009b).
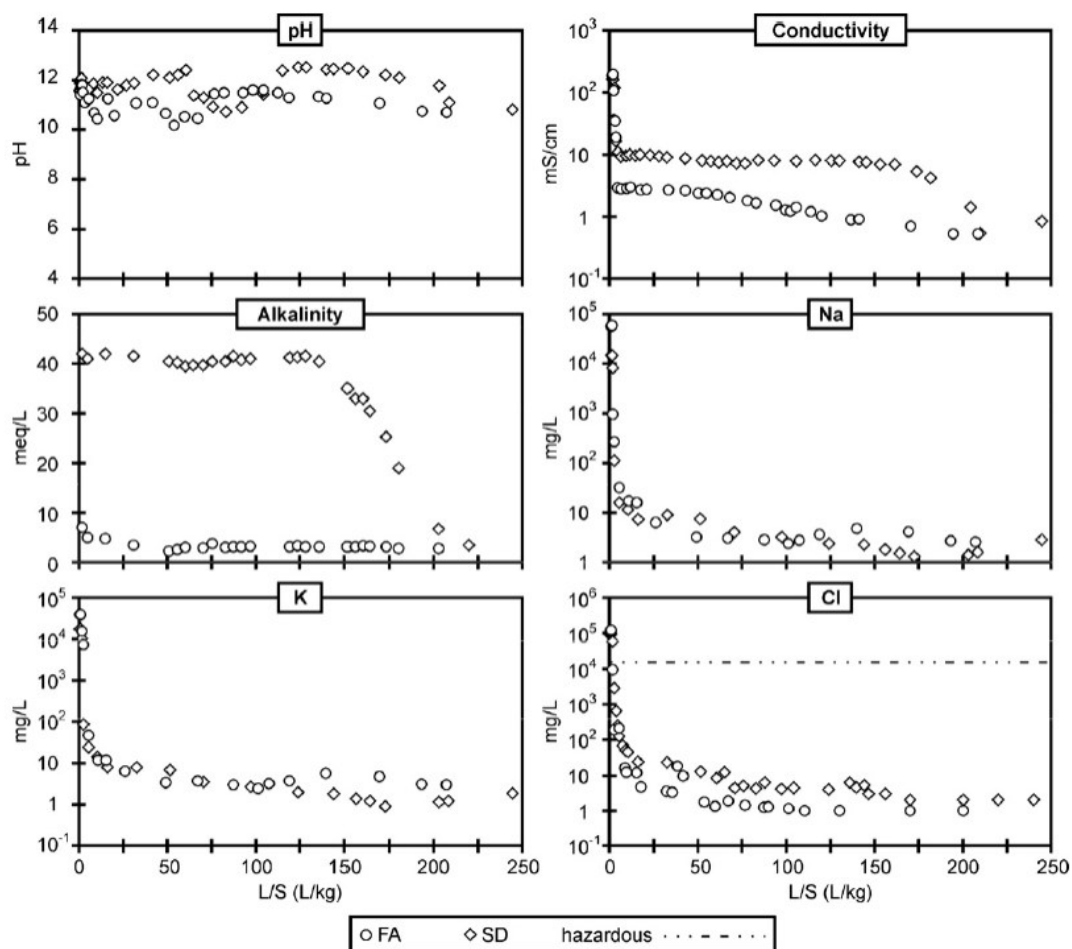

Figure 5. High initial leaching of alkalis and Cl from the APC residues during a long-term column leaching experiment. The pH, conductivity and alkalinity patterns are also depicted (Hyks et al., 2009b).

2.4.3 Waste rock

The mining sites and the waste rock repositories represent possible sources of environmental (e.g., groundwater) contamination via the production of acidity originating mainly from the oxidation of sulphides (Strömberg and Banwart, 1999; Poaty et al., 2021). The acid mine drainage (AMD) usually contains high concentrations of metals and sulphates (Poaty et al., 2021). The laboratory column

leaching experiment (using large columns) on a waste rock from the Aitik copper mine in Sweden was carried out by Strömberg and Banwart (1999). The oxidation of sulphides caused a decrease in pH, resulting in stronger weathering of primary silicate minerals (more information below). High average concentrations of Zn (18 mg/kg) and Cu (36 mg/kg) in the eluate were observed as these elements are present in the dissolving sulphide minerals. A large flux of sulphate accompanied the sulphide oxidation; almost 1 g/kg of sulphate was produced on average. In the study by Poaty et al. (2021), Ni-rich waste rock (composed predominantly of anorthosite and hemo-ilmenite (Fe_2O_3-$FeTiO_3$) gangue) from Lac Tio mine, Canada, was subject to column tests to assess the efficiency of Ni capturing within the waste rock storage management. Although the Ni-containing sulphides are subject to oxidation, these rocks are not a source of AMD in the long term, and Ni is efficiently controlled by sorption and Ni hydroxide precipitation. The research showed that Ni and sulphate (the two most important contaminants) leaching is highly dependent on the L/S ratio (small volumes of water poured into the columns caused higher concentrations of the leachate in comparison with large volumes). The highest observed concentrations of nickel and sulphate in the eluate were 4.5 mg/L and 1500 mg/L, respectively (Poaty et al., 2021).

2.5 *Laboratory leaching vs weathering in the field*

Leaching properties determined by a single batch test can hardly be interpreted as an exact simulation of the material's behaviour in the field where the conditions may significantly differ from the scenario being simulated (van der Sloot et al., 2001; Kosson et al., 2014). As a result, based on the leaching results, the incorrect waste classification can be made (van der Sloot et al., 2001; Kosson et al., 2002), leading to either unnecessary placement of the waste to hazardous waste repositories or, on the contrary, to underestimation of the waste toxicity, thereby increasing the risk of the environmental contamination (Kosson et al., 2002).

Under the field conditions, the waste material is subject to phenomena that are not fully simulated by the leaching tests (Hage and Mulder, 2004), such as contact with atmospheric gases, variability of water flow (van der Sloot et al., 2001; Freyssinet et al., 2002; Kosson et al., 2014) or influence of surroundings having properties distinct from the observed waste (Kosson et al., 2002; Souter and Watmough, 2017). The effect of such phenomena can result in substantial differences in factors controlling leachability, such as pH or redox, compared to leaching tests, where these parameters are predominantly dictated by the material itself. It should also be mentioned that laboratory leaching is carried out under fully saturated conditions, whereas, e.g., in disposal sites, the material undergoes wetting and drying cycles corresponding to precipitation events (Fällman and Hartlén, 1994).

2.5.1 *Observations*

Freyssinet et al. (2002) describe a significant difference between the eluates collected from the pores inside an MSWI bottom ash heap (which could be compared to laboratory leachate) and the eluates at the outlet. In the leachate leaving the heap, the decrease in pH and concentrations of some trace metals occurred as a result of *carbonation* (i.e., precipitation of carbonates) in contact with the atmosphere causing "self-regulation" of the system. Lead and Zn were efficiently trapped in the newly formed mineral phases, mainly carbonates. Also, Al hydroxides and sulphates were observed as common newly-precipitated phases. In contrast, Cu, the most important metal contaminant, was exported out of the heap in the form of a chloride complex (Freyssinet et al., 2002).

The experiment by Fällman and Hartlén (1994) compared the natural weathering of various mineral wastes in large-scale lysimeters with laboratory column tests. The same materials exhibited significant pH dissimilarities between the percolates from the field experiments exposed to the atmosphere and the laboratory leaching experiments where synthetic rain (pH 4) was used as the leachant. The comparison of pH development between laboratory and field leaching of the observed mineral wastes is depicted in Figure 6. During dry periods, coarser-grained materials were completely unsaturated in the lysimeter study and could fully interact with the air. Under atmospheric conditions, wood ash and steel slag produced leachates with pH 9–10, which were thus not as strongly alkaline as in the columns where the pH was rather dictated by the materials themselves. Dissolved atmospheric CO_2 may cause such a

decrease in pH in the alkaline leachates via precipitation of carbonates. Blast furnace slag containing initial large amounts of sulphides showed a steep increase in acidity down to pH 4 in the lysimeter study, caused primarily by oxidation of reduced sulphur species (while pH in the column was around 12). Despite that, reduced conditions were still detected in this leachate. Sulphides, unstable under atmospheric oxidising conditions, represent a source of proton causing a decrease in pH, which leads to increased solubility of most constituents of concern, especially metals. The pH values obtained from MSWI bottom ash leaching were comparable for both leachates (Fällman and Hartlén, 1994).
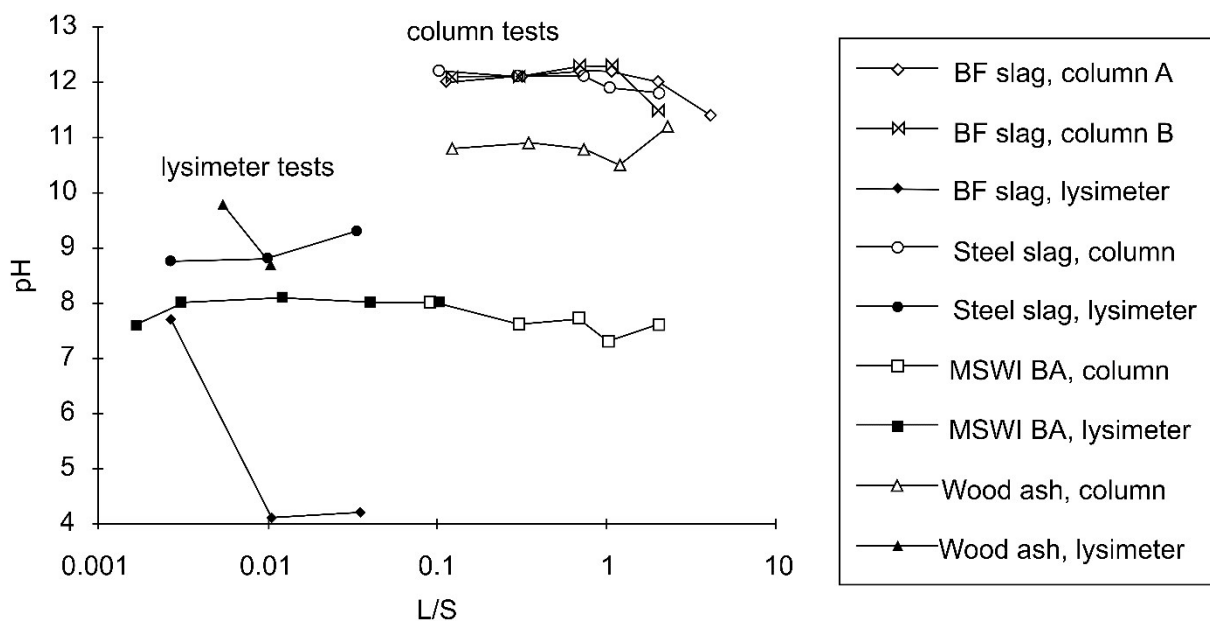

Figure 6. The pH evolution as a function of L/S for leachates of various waste materials. "Column" patterns represent laboratory leaching tests, "lysimeter" ones correspond to leachates obtained from large lysimeters from the in-situ experiment (Fällman and Hartlén, 1994).

Similar results were obtained from the above-mentioned field-simulating leaching experiment by Strömberg and Banwart (1999) on the Aitik copper mine (Sweden) sulphide-rich waste rock. In the large irrigated column reactors with prevailing oxidising conditions, the pH rapidly dropped when the weathering of the primary sulphides outweighed the acidity-consuming processes, primarily $CaCO_3$ dissolution and silicate mineral weathering. The carbonate minerals were almost completely consumed, and the silicate weathering rates increased during the experiment via protonation of the surfaces (still representing partial acidity control). Under the low pH conditions, keeping at 3–3.5, the major contaminant metals, Cu and Zn, were more easily released from the less soluble primary minerals and were not efficiently retained by the secondary phases and remained as dissolved species in the solution. The most of precipitates corresponded to ferric oxyhydroxides minimally enriched in the toxic metals; besides, small amounts of jarosite and gypsum were observed (Strömberg and Banwart, 1999).

Nevertheless, Strömberg and Banwart (1999) admit that the full-scale field situation may substantially differ from the column experiments as the low temperatures and the deposition of rather large rock particles (boulders) limit the weathering of the minerals. Also, difficulties in the gaseous O_2 transport through the whole volume of the deposited rock could lead to lower oxidation of sulphides. The preferential flow and co-deposition of the mineral waste with a neutral rock (consuming its own acidity) would influence the final drainage flow (Strömberg and Banwart, 1999).

Drainage from a Cu-Ni slag pile in Sudbury, Ontario, Canada, observed by Souter and Watmough (2017), showed slightly higher pH values in comparison with a column leaching test of the same material (exposed to the air). The increase in pH happened probably owing to the in-situ influence of the co-deposited alkaline smelting additives (such as lime) and also due to dilution by another water source, whose chemical composition was influenced by the surrounding geological environment and by the soil, both consuming acidity and producing exchangeable cations. Higher Na and Mg concentrations in the pond (compared to the column leaching) can be explained by this process. Metal concentrations in the runoff pond outside the slag pile were comparable with the column experiment; however, binding onto organic matter and precipitation of metal-bearing secondary minerals as a result of increased pH substantially restricted the presence of free metal species in the water (Souter and Watmough, 2017). The comparison of the chemistry of leachates from the column experiment and the runoff pond is shown in Table 4.

Table 4. Comparison of bulk chemistry of Cu-Ni metallurgical slag and leachates from the laboratory column experiment and the drainage pond collected in the field. The values exceeding provincial water quality objectives are indicated in bold. <DL = under detection limit (modified from Souter and Watmough, 2017).

Slag chemistry (mg/kg)		Leachate chemistry (mg/L)	
		Column experiment	Drainage pond
pH		**5.4 ± 0.17**	7.7 ± 0.21
S/SO$_4$	7200 ± 1000	3.6 ± 0.35	170 ± 3.9
Al	9100 ± 1800	**0.15 ± 0.049**	**0.049 ± 0.010**
Fe	140,000 ± 25,000	**1.2 ± 0.41**	0.010 ± 0.0025
Ni	1100 ± 130	**0.94 ± 0.14**	**0.57 ± 0.073**
Co	750 ± 160	**0.11 ± 0.015**	**0.014 ± 0.0022**
Cu	1100 ± 140	**0.25 ± 0.047**	**0.0033**
Zn	240 ± 52	**0.059 ± 0.010**	**0.12 ± 0.0076**
Pb	50 ± 5.7	<DL	0.00019
Cr	15 ± 1.9	<DL	0.00046
Mn	220 ± 48	0.043 ± 0.010	0.055 ± 0.0076
Mg	3300 ± 1200	0.52 ± 0.059	3.9 ± 0.19
Na	2000 ± 440	3.0 ± 0.39	17 ± 1.4
Ca	19,000 ± 4000	9.8 ± 1.4	11 ± 1.4
K	1500 ± 370	5.2 ± 1.8	5.3 ± 0.34

The organic complexation and biological activity represent natural processes that may enhance the mobility of metals (Pareuil et al., 2010; Mikoda et al., 2018). In comparison to EN 14405 column test, an increased metal leaching from a Mn-rich slag was detected in the in-situ reactor simulating deposition of the uncrushed slag in the soil environment for one year. The scheme of the in-situ experiment is shown in Figure 7; a plastic box with the slag was drained by a collector box underneath (separated by PVC retention mesh), all buried in the soil. The leachate was collected continuously up to the L/S of 8. Although the dissolution of primary phases was minimal since the alteration features on the slag surfaces were not observed, the finest fraction of the slag was possibly completely dissolved while the weathering could be enhanced by complexation with the organic ligands. The presence of the alkaline slag also caused an increase in pH and mobilisation of both organic matter and soil colloids in the vicinity of the waste, causing greater leaching of Si, Al, Ca and Fe present in the soil. Also, a significant proportion of the released mass of Cu was leached indirectly from the soil (due to a high affinity with the organic matter). In the eluates from the column tests, substantially lower metal concentrations were observed for any L/S ratio. Nevertheless, even the total masses of metals leached in the in-situ experiment were rather low, 1.9 ± 0.3 mg/L for Mn (in the filtered fraction), lower than 0.8 mg/L for Cu, and lower than 0.2 mg/L for Ni and Zn (Pareuil et al., 2010).
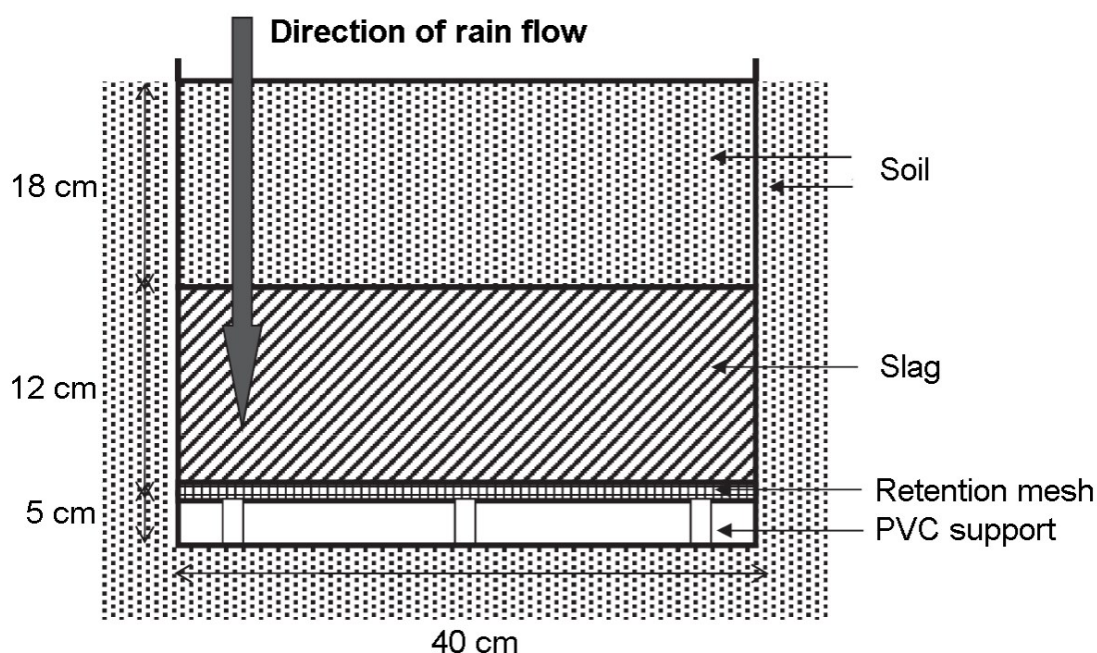

Figure 7. Scheme of the in-situ experiment evaluating the behaviour of the Mn-rich slag in contact with soil (modified from Pareuil et al., 2010).

Generally, the concentrations of mobile metals and metalloids in eluates tend to be lower in the field (Kosson et al., 2014) due to natural processes such as dilution (Souter and Watmough, 2019; Tyszka et al., 2021), carbonation (Freyssinet et al., 2002; Hage and Mulder, 2004; Kosson et al., 2014) and precipitation of other secondary phases, and also sorption onto reactive surfaces (Ettler and Vítková, 2021). However, as we could see above, this is not always the case. The effect of organic and inorganic

acids, the presence of mobilising ligands, or the microbial activity can contrarily result in higher leaching of contaminants (Mikoda et al., 2018). Some highly organic environments do not allow the formation of secondary phases, for example, the hydrous ferric oxides (HFO), because the leached Fe is effectively complexed with the organic ligands (Ettler and Vítková, 2021). The exact behaviour of a particular mineral waste is highly dependent on its mineralogical (and chemical) composition and the storage scenario (Kosson et al., 2002). The processes occurring in the full-scale (field) conditions are rather complicated, and the view provided by the field experiments may be very useful for understanding the real-life behaviour of waste (Pareuil et al., 2010; Ettler and Vítková, 2021).

2.5.2 *Complex approach to determine the waste leachability*

The laboratory tests should be considered only as a part of a more complex, tiered evaluation workflow, as pointed out by Kosson et al. (2002). Combining laboratory pH- or L/S-dependent leaching tests and site-specific information can provide a more robust prediction of elements released over the defined time interval (Kosson et al., 2002). For the scenarios not satisfactorily supported by the full-scale data, geochemical modelling is used as an interpretation tool for the results obtained from the leaching tests (Hyks et al., 2009a, b), especially within the assessment of long-term leaching (Hyks et al., 2009b). Geochemical modelling helps to estimate which mineral phases controlling constituent solubility are present and to assess how sorption onto reactive surfaces or complexation with organic matter and other ligands may affect the total amount of contaminant released or attenuated (Kosson et al., 2002). Moreover, experimental data are needed to set up and validate the models (Hyks et al., 2009a). Despite all efforts to predict the material's future performance, still, none of these predictions can be considered perfect (van der Sloot et al., 2001).

2.6   Metallurgical slags

Slags are waste materials produced by the pyrometallurgical processing of primary ores (primary slags) or pyrometallurgical recycling (secondary slags) (Ettler and Johan, 2014). Metallurgical slags are solid silicate melts having quite variable chemical and mineralogical compositions (Tyszka et al., 2021). Important volumes of slags (millions of tons) are produced yearly (Komnitsas and Zaharaki, 2009; Pareuil et al., 2010). The slag casts shown in Figure 8 were formed by tapping the liquid slag melt into ladles and its subsequent cooling. The slags are generally considered not very reactive and thus do not pose a substantial threat to the environment (Pareuil et al., 2010; Ettler and Johan, 2014; Mikoda et al., 2018). However, in some cases, they can be potentially harmful (especially non-ferrous slags), e.g., when they are exposed to extreme conditions, such as acid rains (Tyszka et al., 2021). This chapter predominantly focuses on the Pb-Zn slags because this type of slag is studied in the experimental part of this work.

Slags from Pb-Zn metallurgy are primarily composed of silicate phases – olivine, clinopyroxene and melilite series, spinel group oxides, and glass enclosing tiny metallic droplets (Ettler et al., 2001, 2002; Ettler and Johan, 2014). Well-formed crystals can usually be found in the core of the slag ladles, as cooling occurred much slower inside than near the rapidly cooled surfaces, where the rapidly formed crystals are characterised by dendritic shapes (Ettler et al., 2001).

Figure 8. Slag ladle casts after solidification (Secondary Pb smelter, Kovohutě Příbram, Czech Republic; Photo: V. Ettler).

2.6.1 Leaching characteristics of Pb-Zn slags

Lead-zinc metallurgical slags are relatively stable owing to the mineralogical composition, compared to matte (being predominantly sulphidic) (Ettler et al., 2001); however, it might still represent a source of contamination. Particularly the release of metals and metalloids from slags under variable conditions is regarded as the highest risk for the environment (Ettler et al., 2001; Pareuil et al., 2010; Tyszka et al., 2021). Table 5 shows concentrations of selected contaminants received from a batch leaching test performed by Ettler and Johan (2014) according to the standard leaching protocol EN 12457-2 and a batch experiment (L/S = 10) extended to 12 years, both conducted on two types of Pb-Zn slags originating from the Příbram smelter (Czech Republic).

Two major processes related to weathering of the slags have been described by Ettler et al. (2001) and include (i) the leaching of glass and (ii) the development of secondary phases (also mentioned by Pareuil et al., 2010 and Souter and Watmough, 2019). Crystalline phases, which contain metals in their structure, are not dissolved to such an extent as the glass hosting small (often <1 μm in size) sulphidic droplets, which are the most important metal carriers (Ettler et al., 2001, 2002). Thus, slags with a higher proportion of glass are considered more hazardous due to their dissolution properties. Apart from the surface layer, the glass filling space between the crystals may also dissolve, leaving skeletons of not dissolved silicates and oxides (Ettler et al., 2001).

Table 5. Leached concentrations of selected contaminants (mg/kg; mean ± standard deviation) after 1 day and 12 years of slag leaching as obtained by the EN 12457-2 leaching test (Ettler and Johan, 2014).

Code	Primary Pb slag (Pb-ore processing)		Secondary Pb slag (Pb recycling)		Limit values (a)		
	1 day [b]	12 years [c]	1 day [b]	12 years [c]	Inert	NH	H
Pb	7.40 ± 6.10	15.3 ± 0.02	0.70 ± 0.10	0.21 ± 0.02	0.5	10	50
Zn	4.65 ± 3.85	**8460 ± 9.0**	0.05 ± 0.00	0.43 ± 0.27	4	50	200
Cu	0.55 ± 0.15	1.74 ± 0.02	0.25 ± 0.05	0.32 ± 0.01	2	50	100
As	0.30 ± 0.06	0.06 ± 0.01	0.01 ± 0.00	0.05 ± 0.00	0.5	2	25
Sb	nd [d]	0.27 ± 0.00	nd [d]	0.58 ± 0.00	0.06	0.7	5
Ba	31.2 ± 26.2	0.15 ± 0.03	**3780 ± 136**	**1930 ± 10**	20	100	300

[a] Limit values for inert, non-hazardous (NH) and hazardous (H) wastes according to EU (2003). Data that exceed the limit values for hazardous waste are in bold.

[b] Mean ± sd for leaching of both coarse- and fine-grained slag fractions.

[c] Mean ± sd for fine-grained slag fraction (n = 2).

[d] nd – not determined.

2.6.2 *Controls on contaminants release from slags*

Secondary phases developed on the weathered surface of the slag fragments are possible concentrators of dissolved metals/metalloids (Ettler and Johan, 2014). The controlling phases commonly include sulphates, carbonates, oxides and complex metal-bearing phases (Ettler and Vítková, 2021; Tyszka et al., 2021). The majority of metals and metalloids (As, Sb, Pb) can be trapped by HFO (Ettler and Johan, 2014; Ettler and Vítková, 2021; Tyszka et al., 2021), which are the most abundant alteration products (Ettler and Vítková, 2021). Adsorption onto HFO represents a crucial mechanism immobilising contaminants within the slag-soil interaction (Ettler and Vítková, 2021).

Dissolution of slag components and subsequent metal release is highly pH-dependent, and pH also determines the formation of secondary phases (Ettler et al., 2002). The pH-dependent leaching curve shape of the individual species depends on the charge of their ionic form. Amphoteric species are most stable under neutral conditions, with the highest leaching at pH extremes, having a V-shaped leaching curve, such as Pb (Ettler and Vítková, 2021). Lead, present in the primary sulphides, is controlled by the precipitation of newly formed anglesite ($PbSO_4$) under acidic conditions and cerussite ($PbCO_3$) under circumneutral-to-alkaline pH conditions (Ettler and Johan, 2014). Cationic species with L-shaped leaching curves, e.g., Zn, Cu, Fe and Ba, are most mobile at acidic pH (Ettler et al., 2002; Ettler and Vítková, 2021). Zinc, partitioned among all the slag phases (silicates, oxides, glass, sulphides) (Ettler and Johan, 2014), is regarded as a significant contaminant due to the limited formation of controlling minerals at neutral pH and its long-term continuous release (Ettler and Johan, 2014; Tyszka et al., 2021). Its controlling secondary phases, zincite (ZnO) or zinc hydroxide [$Zn(OH)_2$], are formed only in a highly alkaline environment (Ettler et al., 2002). Substantial leaching of Ba from the secondary slag was observed during long-term batch leaching experiments by Ettler and Johan (2014) despite massive precipitation of secondary baryte (pH was ca. 8.5). The leaching curve of anionic species looks relatively flat, with slightly higher leaching in lower pH, arsenic (As) is a representative of such anionic specie (Ettler and Vítková, 2021).

2.5.3 *In-situ weathering of slags*

Slags are often stored at open-air disposal sites, piled in heaps, where they are subject to atmospheric weathering (Seignez et al., 2008). Undisturbed slag piles whose release of contaminants is efficiently controlled by the secondary phases represent the best management option (except a safe deposition on an isolated disposal site). However, during some scenarios when the slag faces extreme conditions, such as acid rain events (Tyszka et al., 2021) or contact of small slag particles with acidic soil (Vítková et al., 2011; Tyszka et al., 2021), the dissolution increases, the secondary phases formation is restricted, and the slag becomes a possible source of contamination (Vítková et al., 2011; Tyszka et al., 2021). Tyszka et al. (2021) studied strongly weathered Zn-Pb slags on the heap in Świętochłowice, Upper Silesian Industrial Region, Poland and conducted leaching experiments on both fresh and weathered slag to determine (i) the conditions leading to such extensive weathering (including silicates) and disintegration

of the slag particles and (ii) the leaching behaviour of the material under these conditions. The slag behaviour within the acid rain simulations (at pH 4) highly resembled the observed weathering in the field; the impact of percolation of acidic waters through the heap was thus probably the main factor of weathering. In this study, a periodic appearance of secondary phases on the surface of the heap was described; during the acid rains, the newly-formed phases were dissolved and the bound metals (such as Pb, Cd and As) were washed away (Tyszka et al., 2021). The combination of chemical and physical weathering resembles a chain reaction; the more the slag particles are disintegrated, the more fresh surfaces ready for weathering are exposed. The gradual disintegration results in a continuous release of contaminants from the slags, for example, Zn or Ba (Souter and Watmough, 2019; Tyszka et al., 2021). Apart from Tyszka et al. (2021), the weathered slags crumbling into a fine-grained material were observed by Souter and Watmough (2019).

3. Material and methods

3.1 Studied material

A secondary Pb slag originating from the Pb smelter in Příbram was examined in the experimental part of the bachelor thesis. Příbram, a well-known mining and metallurgical site, is of interest among researchers primarily because of the long-term mining and processing activities and related environmental impacts.

3.1.1 Brief history of mining and metallurgy in Příbram and its surroundings

The presence of lead-silver ores in the Příbram region was probably noticed already by the Celts who inhabited Central Europe several hundreds of years BC. Few archaeological findings prove the occurrence of mining and smelting activities during the Early Middle Ages (Ettler et al., 2001; Kunický and Vurm, 2011). The first written mention of metallurgy works in the district dates back to 1311; by that time, small-scale shaft furnaces were used, processing the ores with a relatively high content of desired metals, mainly silver and lead (Kunický and Vurm, 2011).

Silver (Ag) was the main focus throughout the whole history of Příbram metallurgy until the 20th century when it was substituted by lead (Pb). Despite the minor importance of Příbram in the Middle Ages and the early modern period compared to the silver mining towns of that time, Kutná Hora and Jáchymov, this region was, in the end, discovered to be an extraordinary deposit of Pb and Ag ores. The total Ag production exceeded considerably that of the other mentioned sites. In total, over 3200 tonnes of Ag and 370 000 tonnes of Pb were produced from the local ores (Kunický and Vurm, 2011).

The golden age of mining and smelting came in the 18th and 19th centuries and brought new technologies, such as blast furnaces. The use of steam engines powering the bellows and coke instead of charcoal as a fuel enabled the temperature in the furnaces to rise, and thus, the metal losses were substantially lower. The refining processes were gradually improved in order to facilitate the separation of the desired components. Throughout the entire 20th century, the smelter faced various technological and economic problems, and Pb production was rather low (Kunický and Vurm, 2011). Primary sulphide ores have been stepwise substituted by the Pb-scrap and its recycling; nowadays, exhausted car batteries represent the majority of materials to be recycled (Ettler and Johan, 2014). In 1999, a modern Varta technology was implemented in the Pb pyrometallurgical recycling facility in the Příbram smelter (Kunický and Vurm, 2011).

Production of pyrometallurgical wastes is closely related to Pb smelting activities; the residues include slags, sulphide mattes and several types of ashes. Historical slags and ashes produced by the Příbram smelter were initially used for terrain levelling in the vicinity of the smelter and subsequently, when there was no further use for them, deposited on the large heaps (Kunický and Vurm, 2011). Later, the possible environmental impact of these deposited materials was further studied (Ettler et al., 2001).

3.1.2 Characterisation of the slag

A secondary slag (originating from Pb-scrap recycling) produced in 2021 by the Příbram smelter was used for this leaching experiment. The bulk chemistry of the slag obtained by silicate analysis and acid digestion, followed by an analysis of major and minor elements, respectively, is shown in Table 6. Analysis was performed in the Laboratories of the Geological Institutes, Faculty of Science, Charles University. The concentrations of FeO and SiO_2 account for most of the slag mass, 36.96 wt.% and 23.63 wt.%, respectively. Elevated concentrations of metals can be observed; for instance, Pb (17.41 g/kg), Ba (7.04 g/kg), Zn (5.51 g/kg), Cr (4.01 g/kg) and Cu (0.87 g/kg).

Table 6. Bulk chemical composition of the studied slag (mean, n=2). <DL = below detection limit.

Major elements (wt.%)		Minor elements (mg/kg)	
SiO_2	23.6	Ag	4.33
TiO_2	2.49	As	36.4
Al_2O_3	4.05	Ba	7040
Fe_2O_3	11.1	Be	<DL
FeO	37.0	Cd	7.05
MnO	1.01	Co	<DL
MgO	0.93	Cr	4010
CaO	7.66	Cu	869
Na_2O	2.32	Ga	<DL
K_2O	0.47	Ge	<DL
P_2O_5	0.22	Mo	138
H_2O^-	0.01	Ni	126
H_2O^+	0.97	Pb	17400
CO_2	0.10	Sb	166
S total	6.06	Sn	462
		Sr	284
		V	147
		Zn	5510

Regarding mineralogical composition, the primary phases present in the slag were identified in the laboratories of the Institute of Petrology and Structural Geology using electron microprobe JEOL JXA-8530F (JEOL, Japan) equipped with field emission gun (FEG) and both electron dispersive X-ray spectroscopy (EDS) and wavelength dispersive X-ray spectroscopy (WDS) which was used for the measurements. Accelerating voltage and beam current of (i) 15kV and 20 nA and (ii) 20 kV and 20 nA were set to measure (i) silicate and oxide phases and (ii) sulphides and metallic phases. The quantitative analysis was then recalculated via stoichiometry of the phases. Figure 9 shows the SEM photo of a polished section prepared from the studied material. Spinel (of mainly magnetite or chromite composition), olivine and glass are the most abundant phases; also, clinopyroxene and various types of

Fe-Mn oxides are present. The matrix glass contains metallic inclusions, predominantly composed of sulphides, namely pyrrhotite and galena.
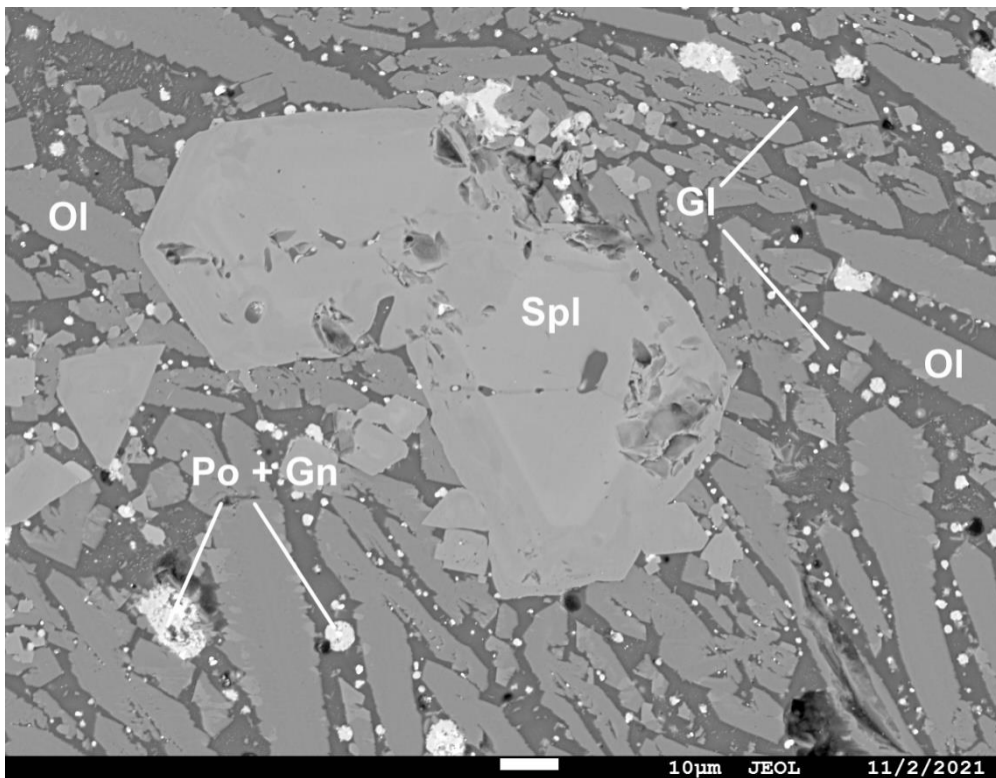
Figure 9. BSE (back-scattered electron) image of Pb-metallurgical slag from Příbram, as obtained by SEM/EDS. Euhedral crystal of spinel (Spl) (chromite) surrounded by needles of olivine (Ol) (predominantly fayalite) embedded in the glass (Gl) matrix hosting inclusions mainly composed of pyrrhotite (Po) and galena (Gn).

3.1.3 Material processing

In order to meet the European standard EN 14405 (2017), it was necessary to carry out the grain size reduction using a jaw crusher so that a fraction over 4 mm accounts for less than 20 % of the sample mass. The granulometry was checked by dry sieving using a set of stainless-steel sieves (Retsch, Germany) with sieve openings of 4 mm, 2 mm, 1 mm and 500 µm. The final grain size distribution is as follows: > 4 mm (7.0 %), 4 mm–2 mm (47.6 %), 2 mm–1 mm (20.1 %), 1 mm–500 µm (9.6 %), < 500 µm (15.8 %).

3.2 Methods

3.2.1 Background of the experiment

During spring 2022, the column leaching experiment was set up by V. Ettler and started for the first time and reached the L/S ratio of 30. Afterwards, the columns were stopped and opened to study the secondary phases precipitated on the surfaces of the slag and quartz sand grains. The mass of the slag in the columns was left to dry out for several months. At the end of 2022, the upper sand layer was replaced, and the experiment was made ready for a restart in January 2023. The main objective of this research is to observe the effect of drying out and a restart of a standardised column experiment on the slag leaching patterns relating to the previous run of the experiment. Only this dataset is discussed in this bachelor thesis. It is nevertheless important to mention that V. Ettler continued this wetting-drying cycle with another set of percolation tests in the spring of 2023.

3.2.2 Laboratory column leaching

We carried out a dynamic leaching experiment on metallurgical slag, following the European standard EN 14405 (2017) guidelines. Two column experiments with the same parameters were run simultaneously so that the results could be compared. The plastic columns with an internal diameter of 5 cm and a height of 30 cm were used; the base and the top part incorporating the inlet and the outlet tube were made of PMMA plastic. The studied material was enclosed between fine quartz sand layers of approximately 1–2 cm serving as natural filters. Exactly 1 kg of the sample was inserted into the column; that means the L/S ratio values are roughly equal to the volume in L of the leachant which had passed through. The column was saturated with the leaching solution (i.e., distilled water) using a volumetric pump and left for 3 days to get equilibrated. After the equilibration period, the pump was started again with the set volumetric flow rate of approximately 12 mL/h, which corresponds to the required linear velocity of 15 cm/d. A PP test tube was used to sample the first 10 mL of the eluate to check the pH. As expected for this type of material, the pH did not exceed the value of 9, and keeping the sampling bottles under an inert atmosphere was not considered necessary. Seven prescribed fractions of the eluate were sampled corresponding to the L/S of 0.1, 0.2, 0.5, 1, 2, 5 and 10. The collection vessels were made of HDPE; the size of the bottle matched the final volume of the currently sampled L/S fraction. The full experiment setup is shown in Figure 10. In the course of the experiment, the volumetric flow rate was checked from time to time using the PP test tubes to be kept at ca. 12 mL/h.

Figure 10. The experimental setup: a) reservoir of the leachant (distilled water), b) volumetric pump, c) layers of quartz sand, d) column with the studied material (Pb metallurgical slag), e) PMMA closings, f) HDPE collection bottle.

3.2.3 Sample processing

Once the desired eluate fraction was complete, it was filtrated using a Millipore Millex-LCR PTFE membrane filter with a pore size of 0.45 μm. Specific conductivity was measured by the Mettler Toledo Seven2Go conductometer equipped with the InLab 738 ISM electrode, calibrated against a conductivity standard of 1413 μS/cm ± 1 % (25 °C). To measure pH and redox potential, the WTW Multi 3620 IDS meter was used with the SenTix 940 electrode and the SenTix ORP-T 900 electrode, respectively.; the pH meter was calibrated against the Hamilton DuraCal buffers with pH values of 4.01 ± 0.01 and 7.00 ± 0.01; the accuracy of the ORP measurements was checked using WTW Redox Buffer RH28 (220 mV/25°C). Alkalinity was determined using the Schott TitroLine Easy automatic titrator equipped with the BlueLine 24 pH electrode; two-point calibration of the device was carried out using the same Hamilton buffers as for pH measurements.

3.2.4 Analytical methods

Subsequently, the sample was prepared for analysis. A combination of inductively coupled plasma optical electron spectrometry (ICP-OES, Agilent 5110, USA) and inductively coupled plasma mass spectrometry (ICP-MS, ThermoScientific X series II, Germany) was used to measure major and minor elements, respectively, in subsamples diluted 10× and 100× with 2% HNO_3. The elements measured by a combination of ICP-OES and ICP-MS were Ag, Al, As, Ba, Be, Bi, Ca, Cd, Co, Cr, Cu, Fe, K, Li, Mg, Mn, Mo, Na, Nd, Ni, Pb, S, Sb, Se, Si, Sn, Sr, Th, Ti, Tl, U, V, Zn and Zr. Determination of anions was carried out by high-performance liquid chromatography (HPLC) (ICS-2000 ion chromatography system, Dionex, USA) in non-acidified samples diluted to < 500 μS/cm.

Certified reference materials NIST SRM 1640a – Trace Elements in Natural Water and NIST SRM 1643f – Trace Elements in Water were used to check the accuracy of measurement with ICP-OES. The latter standard was also used for quality control/quality assurance (QC/QA) procedure during the ICP-MS analysis. In Table 7, the certified values are compared with the measured ones. Geochemical

speciation modelling in PHREEQC, version 3 (Parkhurst and Appelo, 2013) was then accomplished for all the sampled fractions to calculate the speciation of individual constituents in the leachate and the saturation indices of potential solubility-controlling phases. Lawrence Livermore National Laboratory database (LLNL.dat) was used for all the calculations. Electron microprobe analyser (EPMA) JEOL JXA-8530F (JEOL, Japan) and scanning electron microscope (SEM) (TESCAN Vega, Czech Republic) were used to observe newly formed mineral phases between the first and second run of the experiment. Raman spectroscopy was used (Renishaw inVia Reflex, Renishaw, UK) to complete the electron microscopy observations with measurements of the secondary phases.

Table 7. QC/QA of the ICP-OES and ICP-MS analysis. The concentrations of macro and trace elements in the NIST SRM 1640a and 1643f are compared to the measured values.

ICP-OES			ICP-MS		
mg/L	certified	measured	µg/L	certified	measured
	SRM 1640a			SRM 1643f	
Ca	5.62 ± 0.02	5.02	Ag	0.97 ± 0.01	1.02
K	0.58 ± 0.00	0.68	Al	134 ± 1.2	60.3
Mg	1.06 ± 0.00	1.06	As	57.4 ± 0.4	55.9
Na	3.14 ± 0.03	3.18	Ba	518 ± 7	495
S	-	1.51	Be	13.7 ± 0.1	14.0
Si	5.21 ± 0.02	4.85	Bi	12.6 ± 0.1	11.4
			Cd	5.89 ± 0.13	6.54
mg/L	certified	measured	Co	25.3 ± 0.2	25.6
	SRM 1643f		Cr	18.5 ± 0.1	18.6
Ca	29.4 ± 0.3	27.5	Cu	21.7 ± 0.7	21.1
K	1.93 ± 0.01	1.98	Fe	93.4 ± 0.8	169
Mg	7.45 ± 0.06	7.09	Li	16.6 ± 0.4	16.0
Na	18.8 ± 0.3	18.6	Mn	37.14 ± 0.6	36.7
S	-	0.32	Mo	115 ± 2	117
Si	-	0.03	Ni	59.8 ± 1.4	58.7
			Pb	18.5 ± 0.1	18.2
			Sb	55.5 ± 0.4	60.1
			Se	11.7 ± 0.1	14.5
			Sn	-	0.014
			Sr	314 ± 19	298
			Ti	-	108
			Tl	6.89 ± 0.04	6.91
			U	-	0.005
			V	36.1 ± 0.3	38.9
			Zn	74.4 ± 1.7	77.4
			Zr	-	0.012

4. Results

4.1 Physicochemical parameters of the eluates

Specific conductivity evolution (Figure 11) was predominantly affected by the higher initial dissolution of primary slag phases, attaining values of 2100 µS/cm for both columns. This parameter significantly decreased during the first L/S fractions; specific conductivity dropped below the value of 500 µS/cm at L/S of 1.
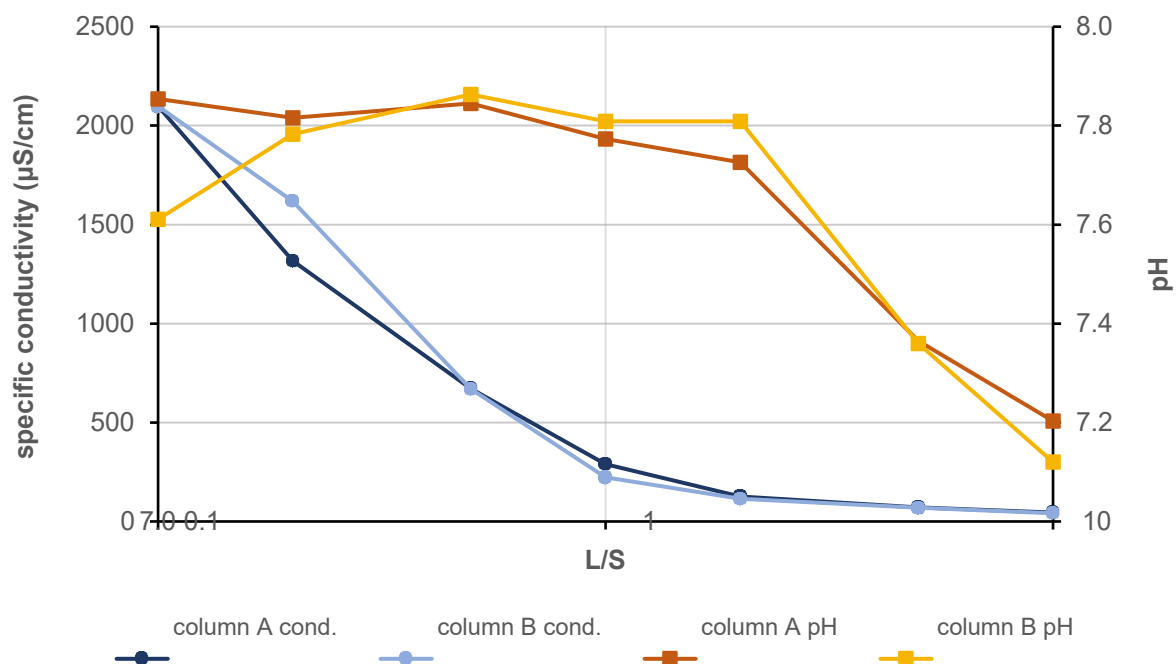
Figure 11. The specific conductivity and pH evolutions.

The pH pattern (Figure 11) in both columns was rather steady, neutral to slightly alkaline (~7.1–7.9). A subtle decrease towards the neutral pH could be observed in the last two eluate fractions. Oxidising conditions prevailed in the course of the experiment (Eh = 400–510 mV).

32

4.2 Release of major and trace elements

The results of the leaching of macro compounds and trace elements from the secondary Pb metallurgical slag during the column test are depicted in Figures 12 to 15. The total sulphur concentrations obtained by ICP-OES measurement were recalculated to SO_4^{2-} and compared with the data from HPLC (Figure 13). The behaviour of all the observed anionic species was similar, with the highest leachate concentrations at the beginning of the experiment, followed by a steep decrease in leaching and
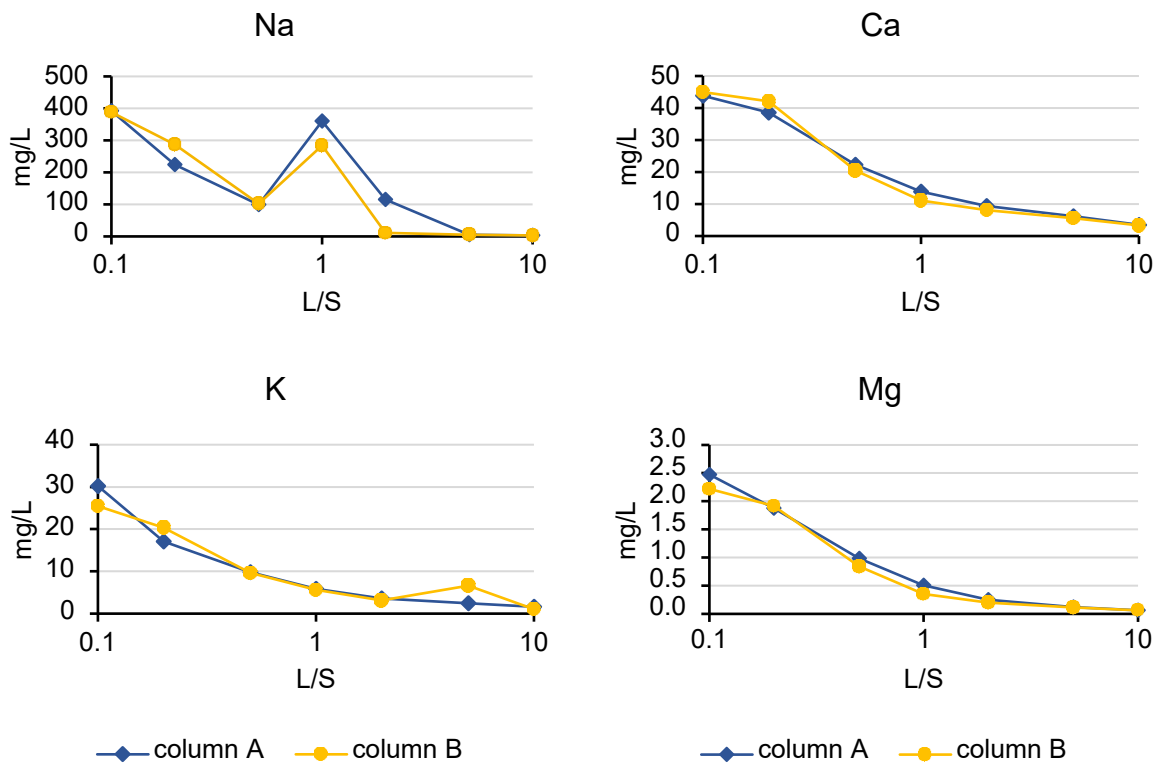
Figure 12. Concentrations of major elements in the eluate (with an exception for S) plotted against L/S ratio.
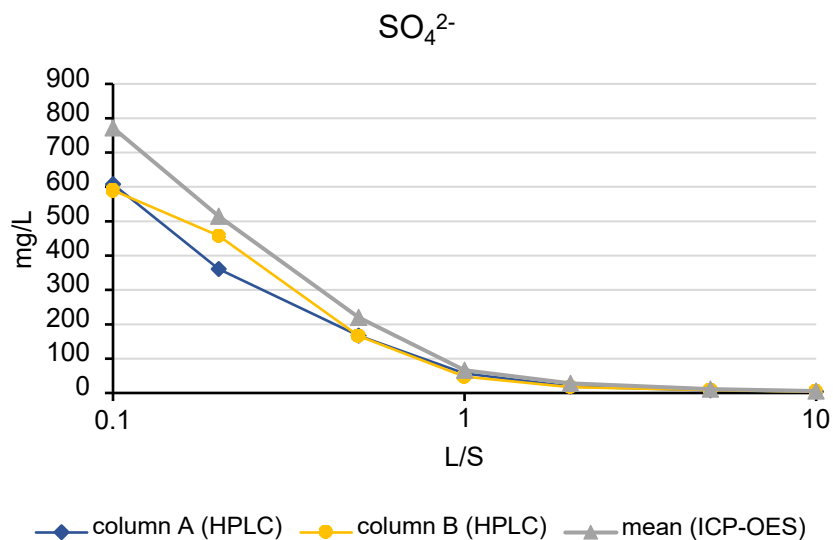
Figure 13. Sulphate concentrations evolution determined by HPLC in comparison with the mean SO_4^{2-} concentrations recalculated from total S (ICP-OES).

subsequent depletion. The concentrations of fluoride and chloride decreased from 5.95 and 160 mg/L to 0.15 and 2.63 mg/L, respectively.

Alkalinity was permanently decreasing during the leaching (Figure 14), from the initial values of ca. 1 meq/L, which corresponds to little more than 60 mg of HCO_3^-/L down to less than 0.2 meq/L.
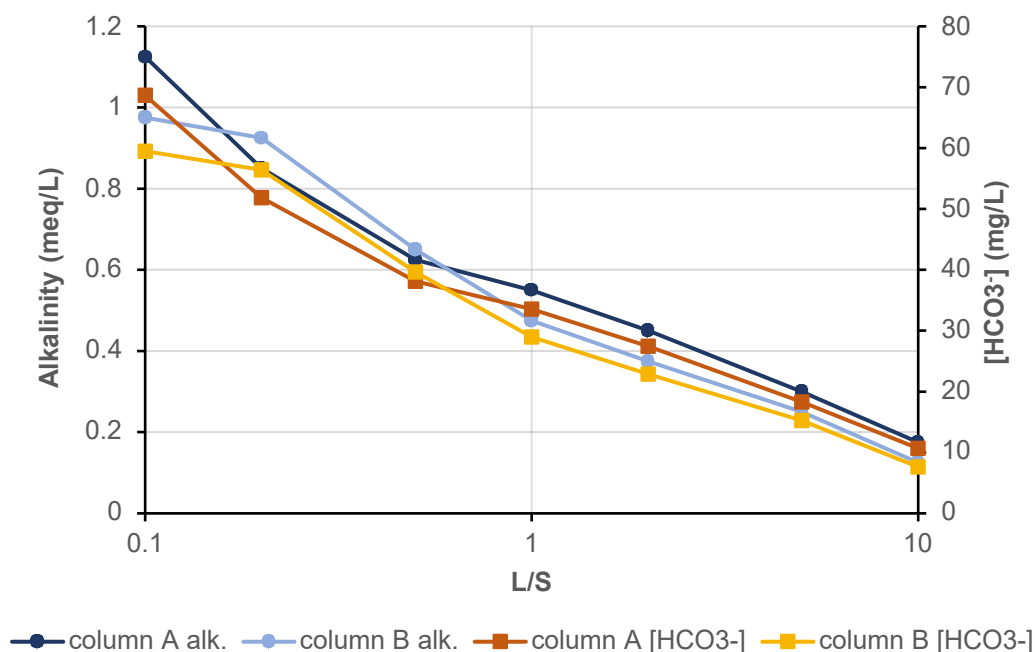
Figure 14. Alkalinity evolution with the corresponding concentrations of HCO_3^-.

In terms of major elements, higher initial concentrations are observed for Na (maximum of 392 mg/L), which is a part of readily-soluble compounds. A peak in concentrations of Na can be found at L/S = 1, whose presence will be further discussed; the concentrations drop to 2.97 mg/L at L/S = 10. The relatively high initial concentrations of sulphur (up to 261 mg/L) and subsequent decrease to 1.86 mg/L agree with the release of sulphate (measured with HPLC), whose concentrations range from 608 to 3.67 mg/L. The continuous decrease in concentrations can be observed for K, with the values ranging from 30.2 mg/L to 1.05 mg/L. Curves of both Ca and Mg decrease more rapidly during the first eluate fractions, with concentrations between 45 mg/L and 3.33 mg/L for Ca and 2.47 mg/L and 0.06 mg/L for Mg (Figure 12).

The majority of trace elements show a gradual decrease in leachate concentrations during the leaching; this does not apply to Ba or Pb, whose concentrations grow higher L/S values (Figure 15). For Ba, the concentrations reach more than twelve times the initial values (max. 932 µg/L). The lowest values (51.1 µg/L) are found at the L/S of 0.2. The concentrations of Pb almost return to the initial levels (which were max. 15.1 µg/L) at L/S = 10 after they are close to zero at L/S = 1 (min. 0.23 µg/L). The concentration peaks of Zn and Mn are shifted to the second sampled eluate fraction (L/S = 0.2), reaching
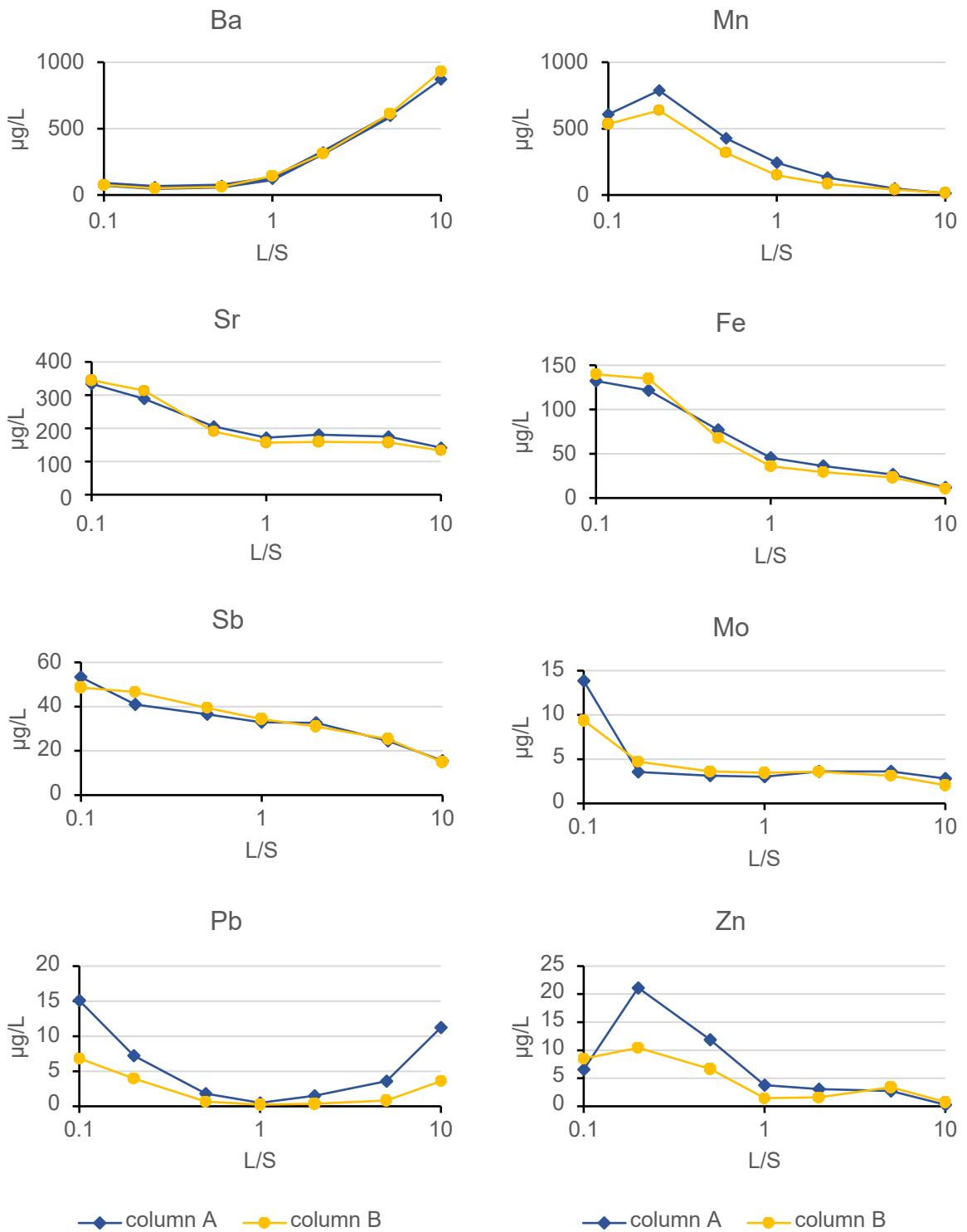
Figure 15. Concentrations of selected trace elements in the leachate plotted against L/S ratio.

values of 21.1 µg/L and 787 µg/L, respectively. The leaching curves of Sr and Sb are similar, continuously decreasing throughout the leaching period. Sr shows a modest drop between the L/S of 0.5 and 2; the concentrations range between 345 and 133 µg/L. Sb concentrations are 14.9–53.3 µg/L. The concentrations of Fe decrease continuously (max. 140 µg/L and min. 10.7 µg/L). After a steep initial decrease from 13.8 µg/L, the concentrations of Mo are relatively constant, around 3.5 µg/L. The minimal value of 2.06 µg/L was reached at the end of the experiment (Figure 15). The total mass of selected major and minor elements released into the leaching solution is shown in Table 8. The values were calculated as the cumulative sum of the mass of the element released in each step of leaching (eluate concentration*volume of the fraction).

Table 8. Total mass of released elements related to the mass of the sample.

major elements (mg/kg)				minor elements (µg/kg)			
	column A	column B	wt.% released*		column A	column B	wt.% released*
Al	0.88	0.79	0.004	Ag	15.5	33.0	0.560
Ca	67.6	61.9	0.118	As	2.31	2.20	0.006
K	29.8	38.5	0.876	Ba	6580	6910	0.096
Mg	1.93	1.7	0.032	Cd	1.48	1.27	0.020
Na	420 S	282	2.040	Cu	6.84	5.62	<0.001
108		105	0.352	Fe	248	217	<0.001
Si	11.9	12.0	0.011	Mn	737	572	0.008
				Mo	32.8	27.5	0.022
				Ni	14.1	16.7	0.012
				Pb	71.6	22.1	<0.001
				Sb	222	220	0.133
				Sr	1630	1500	0.552
				Ti	326	295	0.002
				Zn	21.0	20.2	<0.001

* weight % of the total content released into the solution, calculated from average concentrations of both columns

4.3 Secondary phases

Using EPMA and SEM, the secondary mineral phases precipitated on the surfaces of slag and quartz grains were identified before starting this experiment. We presume that similar phases are responsible for the contaminant release controls within the second run of the column experiment. Iron oxyhydroxides principally composed of ferrihydrite [$Fe(OH)_3$(am)], lepidocrocite (γ-FeOOH) and goethite (α-FeOOH), represent the most common secondary phase, forming continuous coatings on the grains (Figure 16b, c). The individual HFO phases were identified using Raman spectroscopy; the Raman bands of ferrihydrite ($\sim$370, $\sim$700 cm^{-1}) corresponded to the values reported by Mazzetti and
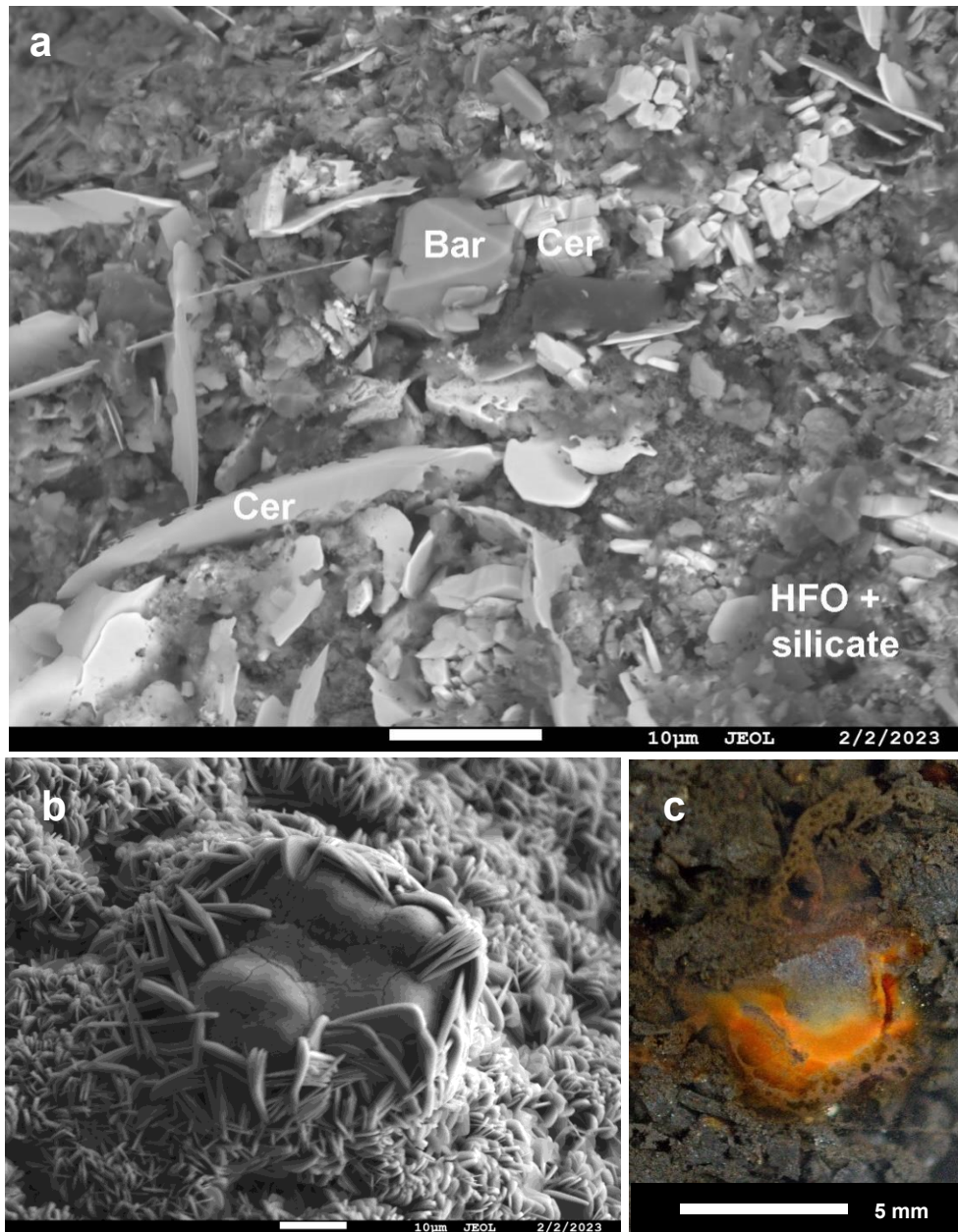
Figure 16. a) BSE (back-scattered electron) image of the secondary phases obtained from EPMA, baryte (Bar), cerussite (Cer) and hydrous ferric oxides (HFO) are visible. b) The tabular crystals of HFO forming a coating on the slag grain. SEM image in SE (secondary electrons). c) The HFO coating at the contact with a slag grain observed during a column experiment (Photo: M. Tuhý).

Thistlethwaite (2002): 370 and 710 cm^{-1}. The detected bands of goethite (249, 300, 389 and 552 cm^{-1}) and lepidocrocite (218, 251, 310, 379, 528 and 650 cm^{-1}) agree well with the reference values for goethite (RRUFF #R120086): 247, 300, 387 and 550 cm^{-1}, and for lepidocrocite (RRUFF #R050454): 216, 250, 303, 380, 525 and 650 cm^{-1} (Lafuente et al., 2015). Additionally, large granular crystals of baryte ($BaSO_4$) and both granular and tabular crystals of cerussite ($PbCO_3$) were observed (Figure 16, a).

4.4   Geochemical modelling with PHREEQC

Both speciation of leached trace elements of interest in the solution (shown in Table 9) and saturation indices (SI) of the main secondary phases, including important solubility-controlling phases, in the course of the experiment (Table 10) are reported.

Table 9. Trace element speciation in the solution for selected trace elements of interest calculated by PHREEQC. The species are ordered according to their abundance.

Ba	Ba^{2+}
Fe	$Fe(OH)_3^0$
Mn	Mn^{2+}, $MnSO_4^0$
Mo	MoO_4^{-2}
Pb	$PbCO_3^0$, Pb^{2+}, $PbOH^+$
Sb	$Sb(OH)_3^0$
Sr	Sr^{2+}
Zn	Zn^{2+}, $ZnSO_4^0$

According to the PHREEQC calculations, Ba, Mn, Sr and Zn occur predominantly as free ionic forms Ba^{2+}, Mn^{2+}, Sr^{2+} and Zn^{2+} over the entire leaching period, minor sulphate complexes of Mn and Zn are present only in the first three eluate fractions. Iron exclusively forms uncharged $Fe(OH)_3$ complexes. Hydroxide forms are also typical for other elements, such as Sb. Uncharged Pb carbonate complexes represent the dominating specie of Pb in the solution. The oxoanionic form of Mo (MoO_4^{2-}) is dominant throughout all the eluate fractions (Table 9).

Table 10. Saturation indices for selected secondary phases as a function of the L/S ratio. Results for both columns are stated separately.

Column A

L/S	0.1	0.2	0.5	1	2	5	10
anglesite ($PbSO_4$)	-2.93	-3.3	-4.1	-4.96	-4.82	-4.46	-4.09
baryte ($BaSO_4$)	1.01	0.73	0.6	0.51	0.51	0.42	0.32
calcite ($CaCO_3$)	-0.32	-0.46	-0.7	-0.95	-1.2	-1.92	-2.55
cerussite ($PbCO_3$)	-0.27	-0.62	-1.24	-1.81	-1.35	-1.18	-0.92
ferrihydrite [$Fe(OH)_3$(am)]	0.71	0.68	0.48	0.25	0.15	0	-0.37
gibbsite [$Al(OH)_3$]	0.83	0.8	0.88	1.1	1.5	1.94	2.08
goethite (α-FeOOH)	5.82	5.78	5.59	5.36	5.26	5.1	4.74
SiO_2(am)	-1.72	-1.74	-1.8	-1.85	-1.88	-1.95	-2.03
smithsonite ($ZnCO_3$)	-3.07	-2.64	-2.88	-3.39	-3.56	-4.12	-5.51
zinc hydroxide [$Zn(OH)_2$]	-3.66	-3.16	-3.26	-3.8	-3.93	-4.66	-5.97

Column B

L/S	0.1	0.2	0.5	1	2	5	10
anglesite ($PbSO_4$)	-3.03	-3.48	-4.55	-5.34	-5.49	-5.03	-4.54
baryte ($BaSO_4$)	0.98	0.75	0.55	0.51	0.47	0.48	0.33
calcite ($CaCO_3$)	-0.62	-0.45	-0.71	-1.06	-1.26	-2.04	-2.82
cerussite ($PbCO_3$)	-0.68	-0.88	-1.65	-2.15	-1.99	-1.87	-1.6
ferrihydrite [$Fe(OH)_3$(am)]	0.73	0.72	0.42	0.14	0.06	-0.07	-0.43
gibbsite [$Al(OH)_3$]	0.91	0.85	0.79	1.03	1.37	1.91	2.06
goethite (α-FeOOH)	5.84	5.83	5.53	5.25	5.17	5.04	4.68
SiO_2(am)	-1.66	-1.69	-1.77	-1.84	-1.88	-1.95	-2.03
smithsonite ($ZnCO_3$)	-3.24	-2.97	-3.1	-3.82	-3.83	-4.11	-5.3
zinc hydroxide [$Zn(OH)_2$]	-4.01	-3.56	-3.48	-4.13	-4.05	-4.58	-5.69

As expected, Fe oxyhydroxides do precipitate during the leaching experiment being major sinks for the released toxic elements (SI varies between 0.73 and -0.43 for ferrihydrite and between 5.84 and 4.68 for goethite; the lepidocrocite is not included in the database). However, the SIs decrease towards the end of the experiment; in the last two fractions, the solution even reaches equilibrium with $Fe(OH)_3$ and is further slightly undersaturated. The solution was slightly oversaturated with regard to both baryte (SI 1.01–0.32) and gibbsite (SI 2.08–0.79). Carbonates did not reach equilibrium throughout the whole experiment; this was valid also for cerussite which was found to be a Pb controlling phase (see Figure 16a). Undersaturation of leachates with respect to anglesite and Zn controlling phases matched the expectations, as the formation of these phases does not occur at circumneutral pH conditions.

5. Discussion

Compared to the preceding column leaching experiment carried out on the same sample of secondary Pb slag, the total leached masses of both major and trace elements were substantially lower. The specific conductivity corresponding to the content of ionic species in the solution decreased from the initial 7370 µS/cm to 68.1 µS/cm after L/S = 20 during the first run of the experiment (while spec. conductivity ranged between 2100 and 41.4 µS/cm within the second run). In the first part of the experiment, the concentrations of Pb were up to 3590 µg/L at the L/S of 0.1, followed by a steep drop down to X0 µg/L after L/S = 0.2 (reaching min. value of 1.65 µg/L) (Ettler, unpublished data). In contrast, the concentrations of Pb start at 15.1 µg/L within the second part of the column test.

It may be assumed that most of the readily-soluble compounds producing constituents such as Na or K, along with the significant sulphidic inclusions in the glass matrix of the slag (releasing both toxic metals/metalloids and SO_4^{2-}), were dissolved during the first run of the experiment. Nevertheless, in the first sampled eluate fractions, especially the concentrations of elements released by the dissolution of readily-soluble compounds exceeded those in the last sampled fraction of the first part of the experiment (which also can be inferred from the specific conductivities). This may be caused by the presence of non-equilibrium in the late stages of the preceding percolation test, as described by Grathwohl and Susset (2009) or Hyks et al. (2009a). During the equilibration period at the beginning of the second run of the experiment, the diffusion-controlled release was enhanced, and the leachate concentrations of the observed elements and compounds were higher after restarting the percolation through the column. This corresponds to the observations of flow interruptions influencing the leaching patterns of trace elements from MSWI bottom ash carried out by Hyks et al. (2009a).

None of the trace elements and compounds reached the limits for inert waste prescribed by the Council decision establishing criteria and procedures for the acceptance of waste at landfills pursuant to Directive 1999/31/EC (EU, 2003), with an exception for fluoride (F-) whose concentrations exceeded the limits for inert waste during the first eluate fractions in both columns but have not reached those for non-hazardous waste. The limit concentrations in column eluate at L/S = 0.1 for inert, non-hazardous and hazardous waste are reported in Table 11. Apart from fluoride, antimony (Sb), with an initial concentration of 53.3 µg/L, was the closest to the limits for inert waste. The long-term batch leaching of a similar secondary slag within the experiment by Ettler and Johan (2014) also indicated the increased leaching of Sb and of Ba; however, compared to Ettler and Johan (2014), the release was rather negligible in this case (the initial concentration of Ba is 0.67 mg/L). The specific L/S dependency of Ba leaching with the gradually increasing concentrations corresponds to the decreasing SI of baryte towards the end of the experiment. However, the baryte precipitates until the L/S of 10 (Table 10).

Similarly to Ettler and Johan (2014), rather unimportant leaching of Pb, Zn, Cu and As, being all below the regulatory limits for inert waste, was observed. Antimony, Pb and As are effectively sorbed onto the

HFO surfaces (Ettler and Johan, 2014); the occurrence of HFO was observed by EPMA and predicted by the geochemical modelling using PHREEQC. Despite that, slightly elevated concentrations of Sb are observed in comparison with Pb and As, whose concentrations are low. The leaching of Zn is also limited. Although the content of Zn in the slag is relatively high (5.5 g/kg), it is supposed to be present predominantly in the less reactive primary phases such as silicates or oxides (Ettler et al., 2001; Ettler and Johan, 2014).

The occurrence of the secondary cerussite forming on the surface of slag particles was expected based on the EPMA observations; however, it was not predicted by the geochemical modelling, exhibiting a saturation index between -0.27 and -2.15 in all the sampled fractions. This happens probably due to very low concentrations of Pb in the eluate. The majority of Pb has already precipitated as cerussite during the previous stages of the experiment or has been sorbed onto HFO. The U-shaped leaching curve of Pb corresponds to the changes in SI of cerussite, however, in a reverse way compared to baryte. The largest decrease of Pb concentrations at L/S = 1 is coincident with the lowest SI of cerussite. This may be caused by the too-low concentrations of Pb, as mentioned above. Probably, the Pb concentrations increase can be connected to the decreasing SI of HFO (ferrihydrite, goethite) and corresponding lower adsorption.

Table 11. Regulation limits for leachate concentrations of hazardous elements or compounds directing the classification of wastes in the case of waste disposal according to the EU (2003) (modified, relevant components selected). The limits are related to the first eluate fraction (L/S = 0.1 L/kg) of the percolation test EN 14405.

mg/L	inert waste	non-hazardous waste	hazardous waste
chloride (Cl^-)	460	8500	8500
fluoride (F^-)	2.5	40	40
sulphate (SO_4^{2-})	1500	7000	7000
As	0.06	0.3	0.3
Ba	4	20	20
Cd	0.02	0.3	0.3
Cu	0.6	30	30
Mo	0.2	3.5	3.5
Ni	0.04	3	3
Pb	0.2	3	3
Sb	0.1	0.15	0.15
Zn	1.2	15	15

As said above, the dissolution of readily-soluble compounds was not excessive as compared with the initial experiment. The extended tailings of Na^+, K^+, Cl^-, SO_4^{2-}, Br^- and F^- indicate that non-equilibrium conditions are observed over the course of the column experiment (Grathwohl and Susset, 2009). The presence of a peak in concentrations of Na at L/S = 1 in both columns cannot be satisfactorily explained. Probably, it may not be imputed to the contamination of the samples because even the following sample fraction (L/S = 2) in column A exceeds the value preceding the peak.

6. Conclusions

Leaching tests are widely utilised for the assessment and classification of waste materials in terms of contaminant release under specific disposal scenarios. The dynamic column leaching tests are advantaged compared to the static batch leaching tests thanks to the possibility of time-dependent leaching observations and to the fact the dynamic is similar to the natural percolation. However, even percolation tests are not a sufficient tool for an exact prediction of the waste material behaviour in the field. External influences affect the leaching patterns, e.g., via dilution of the leachates or precipitation of secondary controlling phases. Both site-specific data and geochemical modelling have to complete the laboratory results to obtain a robust projection.

A column leaching test according to the EN 14405 European standard was carried out to assess the environmental risk related to contaminant release from a secondary Pb metallurgical slag. The column test was also used to compare the results with a preceding column percolation experiment on the same sample and to depict the role of wetting-drying cycles on the contaminant leaching. Although the slag contains a significant amount of toxic elements, such as 17.4 g of Pb per kilogram, the total amount of these elements released is low, only 71.6 µg of Pb per kilogram, and the material is within the regulatory limits for non-hazardous waste. Barium and Sr were the most leached trace elements from the slag. Compared to the first run, the eluate concentrations of both major and trace elements in the corresponding leachate fractions were substantially lower (e.g., more than 200× for the initial release of Pb). Using geochemical modelling, the formation of secondary phases [especially HFO and baryte $(BaSO_4)$] controlling the release of some toxic elements was described. Cerussite $(PbCO_3)$, a solubility-controlling phase for Pb under the circumneutral pH conditions, was undersaturated during the leaching period but was observed by SEM/EDS in the leached slag. Drying the sample and restarting the experiment resulted in (i) higher initial leaching of the constituents like Na^+, Cl^- and F^- after the equilibration period, compared to the last eluate fractions of the preceding part of the experiment (ii) lower leaching of trace elements that were efficiently immobilised by the precipitation of secondary phases formed during the first run of this column experiment.

References

CEN/TC 444 – Environmental characterization of solid matrices. CEN, Brussels. https://standards.cencenelec.eu/dyn/www/f?p=205:7:0::::FSP_ORG_ID:2046877&cs=1C379FCFCAAF69B55CD86BA254B8F2F7F

EN 12457 (parts 1–4), 2002. Characterisation of waste. Leaching. Compliance test for leaching of granular waste materials and sludges.

EN 14405, 2017. Characterisation of waste – Leaching behaviour test – Up-flow percolation test (under specified conditions). CEN, Brussels.

EN 14429, 2015. Characterisation of waste - Leaching behaviour test - Influence of pH on leaching with initial acid/base addition. CEN, Brussels.

EN 14997, 2015. Characterisation of waste - Leaching behaviour test - Influence of pH on leaching with continuous pH control. CEN, Brussels.

EN 15863, 2015. Characterization of waste - Leaching behaviour test for basic characterization - Dynamic monolithic leaching test with periodic leachant renewal, under fixed conditions. CEN, Brussels.

Ettler, V., Legendre, O., Bodénan, F., Touray, J-C., 2001. Primary phases and natural weathering of old lead–zinc pyrometallurgical slag from Příbram, Czech Republic. Can. Mineral. 39, 873-888.

Ettler, V., Mihaljevič, M., Tourey, J-C., Piantone, P., 2002. Leaching of polished sections: an integrated approach for studying the liberation of heavy metals from lead-zinc metallurgical slags. Bull. Soc. Géol. France 173(2), 161–169.

Ettler, V., Johan, Z., 2014. 12 years of leaching of contaminants from Pb smelter slags: Geochemical/mineralogical controls and slag recycling potential. Appl. Geochem. 40, 97–103.

Ettler, V., Vítková, M., 2021. Slag Leaching Properties and Release of Contaminants, in: Piatak, M. N., Ettler, V., Metallurgical slags: environmental geochemistry and resource potential. Royal Society of Chemistry, Cambridge, pp. 151–173.

Ettler, V., Mihaljevič, M., Culka A., 2023. Contaminant release from massive copper metallurgical slags: Insights from long-term monolithic leaching tests. Chemosphere. 335, 139079.

EU, 2003. Council decision of 19 December 2002 establishing criteria and procedures for the acceptance of waste at landfills pursuant to Article 16 of and Annex II to Directive 1999/31/EC. Off. J. Eur. Commun. L11, 27–49.

Fällman, A-M., Hartlén, J., 1994. Leaching of slags and ashes - controlling factors in field experiments versus in laboratory tests. Stud. Environ. Sci. 60, 39–54.

Freyssinet, Ph., Piantone, P., Azaroual, M., Itard, Y., Clozel-Leloup, B., Guyonnet, D., Baubron, J.C., 2002. Chemical changes and leachate mass balance of municipal solid waste bottom ash submitted to weathering. Waste Manage. 22, 159–172.

Garrabrants, A. C., Kosson, D. S., DeLapp, R., van der Sloot, H. A., 2014. Effect of coal combustion fly ash use in concrete on the mass transport release of constituents of potential concern. Chemosphere. 103, 131–139.

Garrabrants, A. C., Kosson, D. S., Brown, K. G., Fagnant Jr., D. P., Helms, G., Thorneloe, S. A., 2021. Methodology for scenario-based assessments and demonstration of treatment effectiveness using the Leaching Environmental Assessment Framework (LEAF). J. Hazard. Mater. 406, 124635.

Grathwohl, P., Susset, B., 2009. Chemical changes and leachate mass balance of municipal solid waste bottom ash submitted to weathering. Waste Manage. 29, 2681–2688.

Hage, J.L.T., Mulder, E., 2004. Preliminary assessment of three new European leaching tests. Waste Manage. 24, 165–172.

Hyks, J., Astrup, T., Christensen, T.H., 2009. Leaching from MSWI bottom ash: Evaluation of non-equilibrium in column percolation experiments. Waste Manage. 29, 522–529.

Hyks, J., Astrup, T., Christensen, T.H., 2009. Long-term leaching from MSWI air-pollution-control residues: Leaching characterization and modeling. J. Hazard. Mater. 162, 80–91.

Komnitsas, K., Zaharaki, D., 2009. 16 - Utilisation of low-calcium slags to improve the strength and durability of geopolymers, in: Provis, J. L., van Deventer, J. S. J., Geopolymers: Structures, Processing, Properties and Industrial Applications. Woodhead Publishing Series in Civil and Structural Engineering, pp. 343–375.

Kosson, D.S., van der Sloot, H.A., Sanchez, F., Garrabrants, A.C., 2002. An Integrated Framework for Evaluating Leaching in Waste Management and Utilization of Secondary Materials. Environ. Eng. Sci. 19, 159–204.

Kosson, D.S., van der Sloot, H.A., Garrabrants, A.C., 2014. Leaching Test Relationships, Laboratory-to-Field Comparisons and Recommendations for Leaching Evaluation using the Leaching Environmental Assessment Framework (LEAF). EPA-600/R-14/061, US EPA, Washington, D.C.

Kunický, Z., Vurm, K., 2011. 700 let hutnictví stříbra a olova na Příbramsku (1311–2011), 225 let Stříbrné hutě - Kovohutí Příbram (1786–2011), Kovohutě Příbram, Příbram.

Lafuente, B., Downs, R. T., Yang, H., Stone, N., 2015. The power of databases: the RRUFF project. In: Highlights in Mineralogical Crystallography, T. Armbruster and R. M. Danisi, eds. Berlin, Germany, W. De Gruyter, pp 1–30.

LEAF, 2022. Leaching Environmental Assessment Framework. Vanderbilt University https://www.vanderbilt.edu/leaching/   (17.12.2022)

Leaching.net, 2007. Relevance of leaching. http://www.leachxs.com/   (11.04.2023)

Mazzetti, L., Thistlethwaite, P. J., 2002. Raman spectra and thermal transformations of ferrihydrite and schwertmannite. J. Raman Spectrosc. 33, 104–111.

Mikoda, B., Kucha, H., Potysz, A., Kmiecik, E., 2018. Metallurgical slags from Cu production and Pb recovery in Poland – Their environmental stability and resource potential. Appl. Geochem. 98, 459–472.

Parkhurst, D. L., and Appelo, C. A. J., 2013. Description of input and examples for PHREEQC version 3—A computer program for speciation, batch-reaction, one-dimensional transport, and inverse geochemical calculations: U.S. Geological Survey Techniques and Methods, book 6, chap. A43, 497 p., https://doi.org/10.3133/tm6A43

Pareuil, P., Bordas, F., Joussein, E., Bollinger, J.-C., 2010. Alteration of a Mn-rich slag in contact with soil: In-situ experiment during one year. Environ. Pollut. 158, 1311–1318.

Poaty, B., Plante, B., Bussière, B., Benzaazoua, M., Thériault, M., 2021. A column study of the impact of layering the different Lac Tio mine waste rock lithologies on drainage water quality. J. Geochem. Explor. 229, 106823.

Seignez, N., Gauthier, A., Bulteel, D., Damidot, D., Potdevin, J.-L., 2008. Leaching of lead metallurgical slags and pollutant mobility far from equilibrium conditions. Appl. Geochem. 23, 3699–3711.

Souter, L., Watmough, S.A., 2017. Geochemistry and toxicity of a large slag pile and its drainage complex in Sudbury, Ontario. Sci. Total Environ. 605-606, 461–470.

Strömberg, B., Banwart, S., 1999. Weathering kinetics of waste rock from the Aitik copper mine, Sweden: scale dependent rate factors and pH controls in large column experiments. J. Contam. Hydrol. 39, 59–89.

SW-846 – Test Methods for Evaluating Solid Wastes. US EPA, Washington, D.C. https://www.epa.gov/hw-sw846

Test Method 1313, 2017. Liquid-Solid Partitioning as a Function of Extract pH Using a Parallel Batch Extraction Procedure. US EPA, Washington, D.C.

Test Method 1314, 2017. Liquid-Solid Partitioning as a Function of Liquid-Solid Ratio for Constituents in Solid Materials Using an Up-Flow Percolation Column Procedure. US EPA, Washington, D.C.

Test Method 1315, 2017. Mass Transfer Rates of Constituents in Monolithic or Compacted Granular Materials Using a Semi-Dynamic Tank Leaching Procedure. US EPA, Washington, D.C.

Test Method 1316, 2017. Liquid-Solid Partitioning as a Function of Liquid-to-Solid Ratio in Solid Materials Using a Parallel Batch Procedure. US EPA, Washington, D.C.

Tyszka, R., Pietranik, A., Potysz, A., Kierczak, J., Schulz, B., 2021. Experimental simulations of Zn–Pb slag weathering and its impact on the environment: Effects of acid rain, soil solution, and microbial activity. J. Geochem. Explor. 228, 106808.

van der Sloot, H.A., Kosson, D.S., Hjelmar, O., 2001. Characteristics, treatment and utilization of residues from municipal waste incineration. Waste Manage. 21, 753–765.

Vítková, M., Ettler, V., Mihaljevič, M., Šebek, O., 2011. Effect of sample preparation on contaminant leaching from copper smelting slag. J. Hazard. Mater. 197, 417–423.

Zhang, M-H., Blanchette, M.C., Malhotra, V.M., 2001. Leachability of trace metal elements from fly ash concrete: Results from column-leaching and batch-leaching tests. Aci Mater. J. 98(2), 126–136.

List of figures

List of tables